ISTITUTO NAZIONALE DI FISICA NUCLEARE

Sezione di Milano

G. Ambrosio, F. Ametrano, G. Bellomo, F. Broggi, L. Rossi, G. Volpini:

PRELIMINARY PROPOSAL OF A Nb$_3$Sn QUADRUPOLE MODEL FOR THE low β INSERTIONS OF THE LHC

PACS: 85.25.+K

PRELIMINARY PROPOSAL OF A Nb_3Sn QUADRUPOLE MODEL FOR THE *low* β INSERTIONS OF THE LHC

G. Ambrosio, F. Ametrano, G. Bellomo, F. Broggi, L. Rossi, G. Volpini
Dipartimento di Fisica dell'Università di Milano, INFN–Sezione di Milano
Laboratorio LASA, via Fratelli Cervi 201, 20090 Segrate (Milano) – I

ABSTRACT

In recent years Nb_3Sn based conductors have shown wide applicability for superconducting magnets in many research areas like high field solenoids for laboratory experiment, for NMR spectroscopy and high field magnets for fusion. Nb_3Sn technology is progressing fast, increasing both technical reliability and availability.

The Nb_3Sn technology, which has a higher critical field than NbTi, seems attractive for IR (Insertion Region) quadrupoles of large colliders. In this paper we propose the construction of a superconducting quadrupole wound with Nb_3Sn cable for a second generation IR inner triplet *low* β quadrupoles, for the Large Hadron Collider at CERN. The *low* β quadrupoles, control the beam focusing at collision points, therefore a gain in term of focus strength and/or coil aperture can increase significantly machine performance.

Two are the main steps for the whole project:
1) design and construction of a 1 metre long quadrupole to demonstrate the actual feasibility, which is the subject of this proposal;
2) study for integration of the quadrupole in the machine and final design of 5 m long quadrupoles finalized to the LHC.

Contents

1 SUMMARY OF THE PROPOSAL

1.1 Frame and Purpose of the Proposal

The CERN-INFN collaboration on superconducting magnets for the LHC has concluded the first step with the successful test in 1994 of the first two 10 m long dipoles, that reached the field of 9.5 tesla and have operational field of 9 tesla at 1.8 K.

The new collaboration, signed at the end of 1994, plans a main activity for the construction of the first LHC 15 m long, curved, prototype dipole. For this prototype the main design responsibility rely on CERN (AT/MA group). INFN has a role of major responsibility in the production and test of the superconducting cable, and in the construction of the coils and of the cryostat.

In the new collaboration there is room also for a development, carried out mainly by INFN, of a superconducting quadrupole which may be an improvement to the low β quadrupoles envisaged at present.

INFN, on proposal by LASA group, has included in its present Five Years Plan an R&D activity on high field (i.e. in excess of 10 tesla) accelerator dipoles and/or quadrupoles wound with Nb_3Sn conductor. The reasons to include this R&D in a real project are :

- the LASA has reached, as a result of a four year activity, a relevant technical capability on the design and construction of Nb_3Sn windings. By the end of the year we will install in LASA a solenoid, able to generate a field of 18 tesla in a 100 mm bore. Few small Nb_3Sn solenoids have been wound and successfully tested at LASA;

- construction of LHC should not stop the European effort for very high field accelerator magnets. Apart from the technological benefits in a view of giant accelerators in the hundreds TeV range, Nb_3Sn windings might become an advantageous solution for small compact accelerators where field over 8 tesla at 4.2 K with short strongly curved magnets may be required;

- the new availability in Europe of a new Nb_3Sn technology yielding a current density suitable for accelerator magnet and very interesting price; it would make sense to explore this conductor in a real coil for our applications (for example this conductor is going to be widely used in the ITER project for fusion and for high field solenoids);

- in the LHC project there is still possibility for use of Nb_3Sn : there are special magnets around the beam collision points which are likely to be changed during the LHC life. An increase of the performances of the inner triplet quadrupoles may positively affect the machine luminosity;

- to acquire, inside INFN, the capability of designing superconducting magnets for accelerators. An effective capability can be gained only with a real project.

The magnet we are proposing fulfils both the interest in Nb_3Sn technology development and possible spin off with practical application for accelerator magnet.

1.2 Technical Proposal

A technical summary of the proposal is reported here, followed by an extensive description with technical detail and inserted into the frame of the present panorama of accelerators and of Nb_3Sn technology.

Coils will be shaped in circular "cos θ" shells, being the alternative rectangular blocks shape decisively less efficient and more difficult to wound at the coil ends. Use of Nb_3Sn conductor calls for fully impregnated coils wound in pair (double pancake technique). The superconducting cable is composed by 36 strands assembled in a trapezoidal shape (Rutherford cable) and has dimension similar to the cable used for the outer layer of the LHC dipole. A prototype length of the cable has already been manufactured with a very promising critical current density $J_c = 1850$ A/mm^2 measured at 10 tesla, 4.2 K *after cabling.*

The model should be at least 1 m long (with possibly 60 cm of straight section length) in order to be effective in testing all construction solutions and to be significant also for field quality measurements in the straight part.

Three different coil design were investigated, all surrounded by the iron return flux yoke:

1. *2S – two shells of Nb_3Sn*

2. *2S + 2S – two shells of Nb_3Sn plus two shells either of Nb_3Sn or of NbTi (in this case called 2S+2T)*

3. *4S– four shells of Nb_3Sn*

The difference between 2S+2S and 4S is mainly that in the last design the outer two coils have the same azimuthal extension as the two inner layers. As detailed in the section dedicated to the quadrupole description, we have rejected the 2S+2S design and

we propose to built either the 2S or the 4S model quadrupole, with a strong preference for the 2S model that is more efficient and closer to an optimized design

A picture of the different coil arrangement of the two proposed designs is shown in fig. 1.

The *2S* is simpler to build and should be regarded mostly as a technologic proof of feasibility. The *4S* design actually has been studied as an extension of the 2S design, with the same conductor, but it is still far from being optimized. For a quadrupole finalized to the *low β* insertions of LHC will be necessary to spend more time on the design, together with CERN, both for a satisfactory optimization and to be sure it is in the right direction for beam optics (higher gradient or larger aperture) and for operation (current and temperature).

It may be surprising that we are not proposing, at this stage of the design, a grading in the current density, i.e. all coil layers are wound with the same cable. As explained in the proper section, Nb_3Sn has less "grading margin" than NbTi and so far we have not found a grading design with a sensible gain in gradient. At present we prefer a "one cable" magnet and concentrate our effort on Nb_3Sn technology and feasibility, leaving the layout optimization for the second step of the project.

LASA QUAD 2Sn 10+4 19 1wde Shim coll-40 iron (2siron.)   07/05/95 16.09
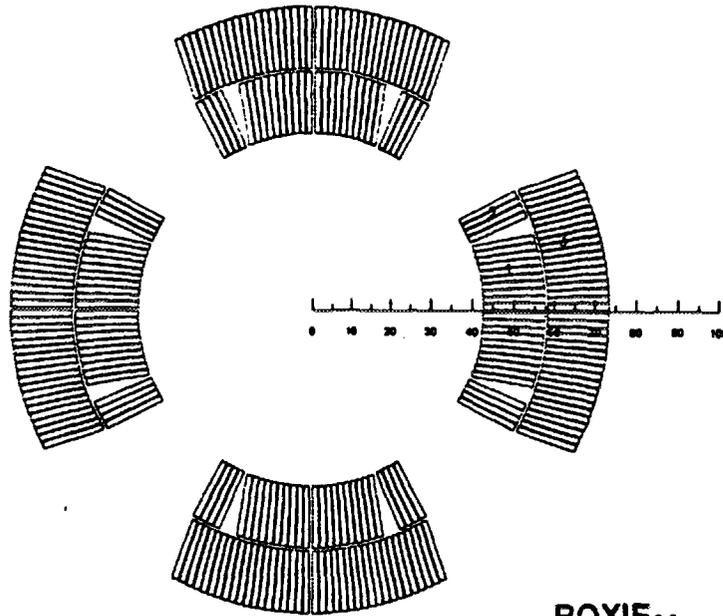
ROXIE₃.₅

LASA QUAD 4Sn 7+7 12+6 23 27 2wed Shim-0.3 coll-40 iron   20/04/95 18.57
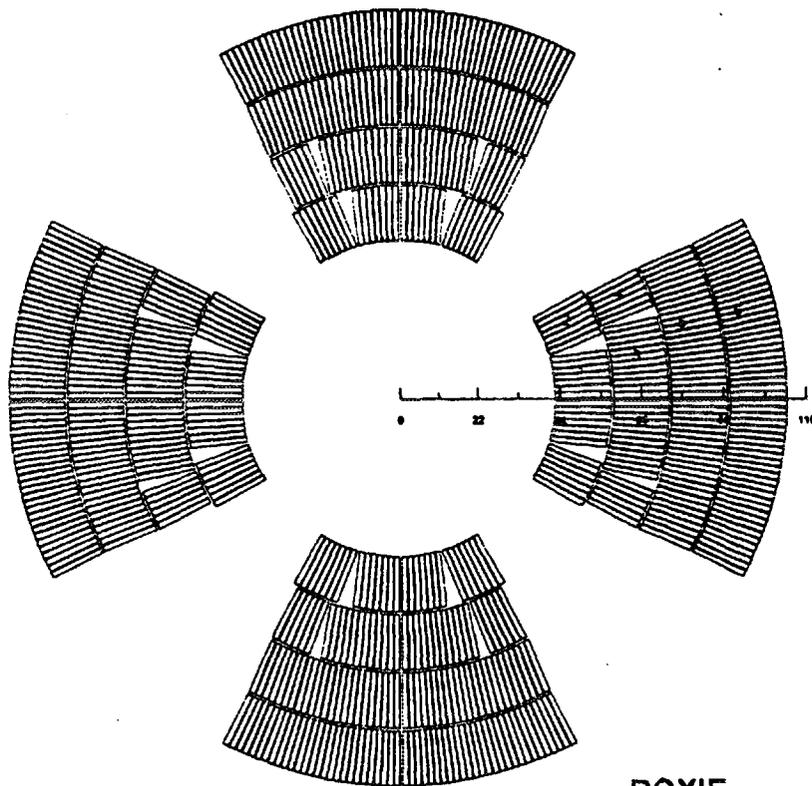
ROXIE₃.₅

FIG. 1: two coil layouts: *2 shells*,top, and *4 shells*, bottom. Coil ϕ_{in}=85 mm.

The aperture of the quadrupole is 85 mm and the nominal gradient is 260 T/m for the 4S design and 240 T/m for the 2S one, when working in superfluid helium at 1.8 K. These numbers should be compared with the nominal gradient of 250 T/m in an

aperture of 70 mm, at 1.8 K, of a 1 m long NbTi *low β* quad model now under test (CERN-Oxford model). Our design, when scaled to 250 T/m, can offer an equivalent coil aperture of 90 mm for the 4S design and 80 mm for the 2S one.

The operating current ranges between 10.5 kA for the 4S and 14.5 kA for the 2S coil layout with corresponding current density in the coils of $J_{overall}$ = 390 to 550 A/mm² (the copper to non copper fraction is about 1:1 in the cable and the insulation is about 30% of the total coil cross section). *Throughout this paper the operating current is taken as ≃93% of the maximum theoretical current as given by short sample measurements.*

A preliminary decision was made to avoid any mechanical contribution from the iron yoke, so special attention was given to the collar design and to the collaring procedure. A collar design where an Al-alloy ring restrains the coil radially and a Ti-alloy wedge is inserted between coils in the so called "pole region" (the iron pole position in classical . electromagnet) is proposed. This collar design should assure that the necessary coil prestress at room temperature is tolerable and increasing with the cool down to restrain conductor movement under the e.m. forces.

The whole magnet cross section of the 2S design is shown in fig. 2, with the wedge and the ring collar.

The collaring will take place by pushing along two orthogonal axes, either against the wedges or the coils. The force necessary for collaring is less than 7 MN/m (700 ton/m) for the 4S and less than 5.5 MN/m (550/m ton) for the 2S. This value can be provided by a custom made press, very low cost, detailed in a dedicated subsection.

The temperature margin is $\Delta T \geq 3$ K for both 2S and 4S designs; this margin is greater than $\Delta T = 1.2$ K of the LHC dipole magnet, also working in superfluid helium; since our coils are fully adiabatic, without the benefit of direct coolant wetting, we think such a margin may be needed for magnet stability; however we expect these coils to show training.

Protection is surely an important issue with such a magnet, especially for the 4S design. Calculation carried out with a numerical code at our lab, suitable for multicoil adiabatic solenoid and modified to describe these coils, indicates that a hot spot temperature can be kept at values below 150-180 K if a simple protection circuit with external dumping resistor (and no coil subdivision) is used. Fixing the dumping resistance value in such a way as to limit the voltage across terminals to 1200 V, and with conservative timing in the quench detection and breaking circuit (10 ms after 200 mV has been developed and 20 ms of time to extinguish the arc of the breaker) and with no quench back effect or help by coupling, we are limited to 190 K which is high but still acceptable. Should detailed calculation be more pessimistic, a coil subdivision with cold shunt resistors can provide adequate protection (at price of more complexity).

In table 1 all the main characteristics of the proposed alternative designs are summarized.

It should be mentioned that so far we have not carried out a detailed analysis of the ends. Since the field accuracy given by the ends is not one of the main item at this point and since interesting developments are going to be carried out in CERN, we think it's worth to investigate the best shape of the ends at project approval. The stability of the conductor at the ends should not be a point really more critical than in the straight part, since in our case the whole winding is impregnated.

2 LAYERS COIL   AI COLLAR (4 STROKES)

IRON YOKE

Ti WEDGE
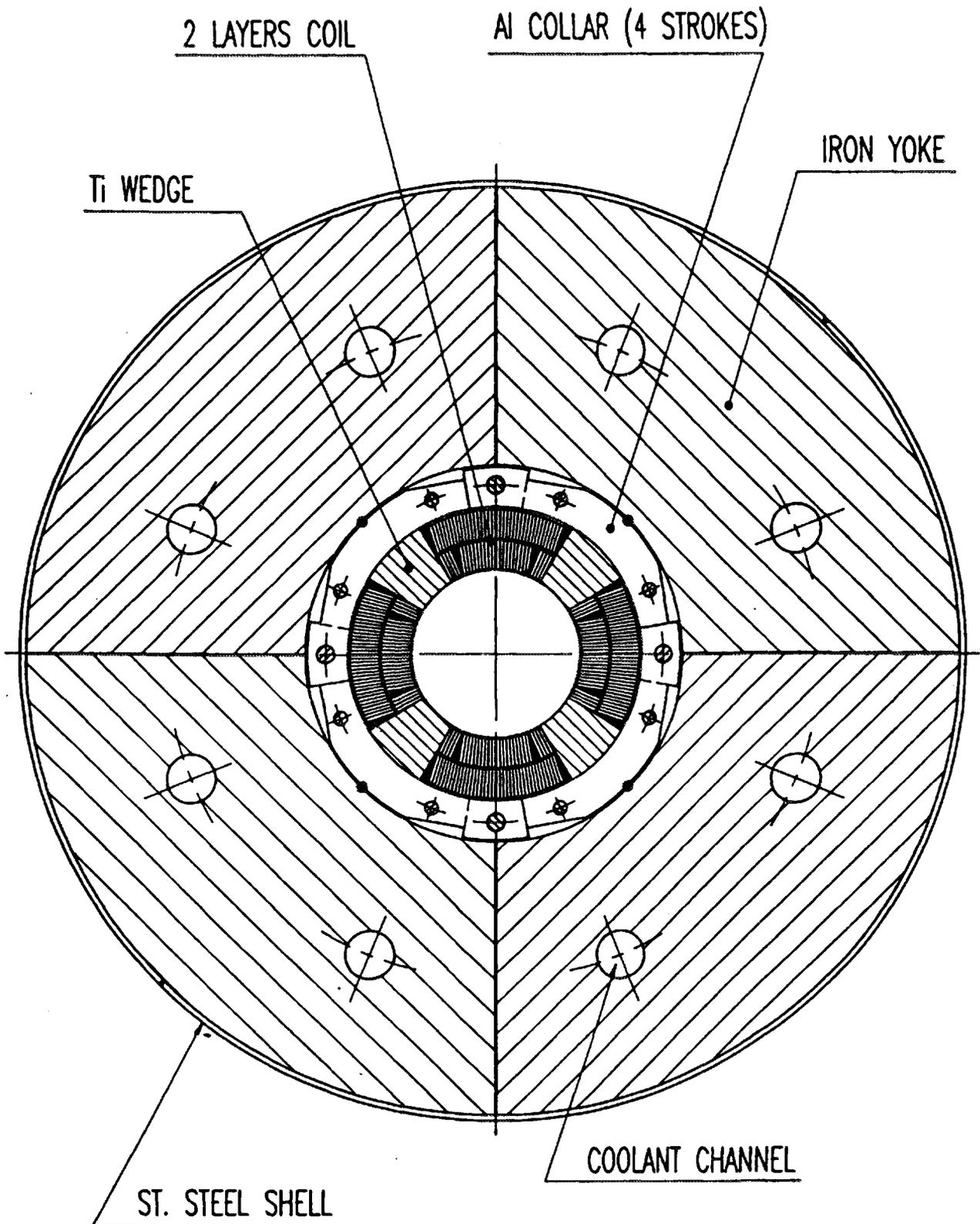
COOLANT CHANNEL

ST. STEEL SHELL

FIG. 2: *2S* design, cross section of the whole magnet.

1.3   Cost and Time Schedule

In table 2 the projected cost of the model is reported. In addition to the usual dummy coils, we believe that it will be worthy to test first a good coil in an arrangement where

TABLE 1: main features of the two designs for the 1 m long quad model

	2 shells	4 shells
coil aperture (mm)	85	85
gradient (T/m)	241	264
250 T/m equivalent coil aperture (mm)	80	90
b_6 at R=1cm (10^{-4})	≤ 0.1	≤ 0.1
b_{10} at R=1cm (10^{-4})	≤ 0.01	≤ 0.01
operating temperature (K)	1.8	
coolant	1 bar (pressurized) static HeII	
peak field on coils (T)	11.7	13.2
superconductor	Nb_3Sn – Internal Tin Diffusion	
J_c non Cu (A/mm^2)	1850 at 10 T, 4.2 K	
α=Cu:non Cu	1.1:1	
cable composition	36 strands, ϕ=0.825 mm	
cable size (mm)	1.34–1.60×15.0	
cable length (m)	300	700
operating current (kA)	14.58	10.41
I_{oper}/I_{max}	93%	93 %
layer numbers	2	4
junctions in low field	1	3
splice in high field	none	none
$J_{overall}$ A/mm^2)	550	390
insulation type	R or S2 glass + epoxy resin impregnation	
insulation thickness (mm)	0.125 azim., 0.250 rad.	
midplane shims (mm)	2×0.3	
inductance (mH)	3.65	22.1
stored energy (kJ)	390	1200
dumping resistance $(m\Omega)$	82	115
temperature margin (K)	4.1	3.1
hot spot temperature (K)	≤ 160	≤ 190
mechanical support	by collars only	
collar ring (Al alloy)	Al 2014-T6	
collar wedge (Ti alloy)	Ti-Al5-Sn2.5	
coil av. prestress after collaring(MPa)	70	50
pressing force (MN)	≤ 2.1	3
pressing style	along X-Y axes	
max. stress of collar	350	200
max. stress of coil	120	150

iron is placed directly over the coil surface. A magnetic mirror, although not perfect because of the strong saturation effects, will give very useful information on the coil behaviour prior to the final magnet construction.

The cost of the test is quoted as if it will be carried out in LASA. For this purpose we have three power supplies that can deliver 10 kAmps up to 6 Volts each. We need to upgrade them with a protection circuit and electronic. There is an available cryostat, ϕ=700 mm and 3 m long, installed for testing superconducting cavities. It is complete

TABLE 2: BREAKDOWN OF THE COST *(MLIT)*

item	2 shells	4 shells
superconducting cable	100	150
coil construction	250	350
collars and collaring	130	150
collaring press	50	70
iron yoke and assembly	110	130
mirror (test coil) construction	70	90
TOTAL OF CONSTRUCTION	710	940
protection circuit	100	100
1.8 K cryogenics	50	50
15 kA current feedthrough	20	20
test of the mirror	30	50
test of the magnet	70	100
magnet measurement system	50	50
TOTAL TESTING	320	370

for a 4.2 K operation but will need to be upgraded for 1.8 K; we need an adequate pair of current leads (15 kA passing through a 1.8 K – 4.2 K separation) and pumping equipment. The other parts of cryogenics (feeding and recovery) are already installed.

The cost of testing can be easily reduced if the test will be carried out at the CERN facility, which has all the necessary equipment, including the magnetic field measurements. In this case, of course, personnel of INFN will actively interact with CERN staff.

The cost breakdown does not include general expenses, such as computing and travelling.

The time schedule for the *2S* mbdel quad will cover three years, i.e. JUNE'95–JUNE'98. It's a tight schedule, considering similar experience with Nb₃Sn dipoles and the fact that it is the first accelerator magnet design for our lab. We believe that strict collaboration with CERN, with Univ. of Twente – prof. H. ten Kate has already given his approval – and with LBL (informal contact has already been made with positive feedback) makes this program a realistic one.

TIME SCHEDULE

- Sept.95 : start with small scale models

- Nov.95–July 96: design and construction of the main tools

- Febr.96 : freezing of the main parameters

- Sept.96 : beginning of coil construction

- Febr.97 : test of the mirror

- July 97 : end of coils construction

- Dec. 97 : end of construction

- Jan.– June 98: test and magnetic measurements

2 PANORAMA OF ACCELERATOR MAGNETS

2.1 Dipole Magnets

The superconducting technology for accelerator magnet is today well developed for fields in the range up to 9 tesla. The present record field is 10.5 tesla, reached in a 1 m long LHC twin dipole model, of 50 mm coil aperture, at 1.8 K after very long training[1] . A field in excess of 10 tesla was also reached, at 1.8 K, by a special 1 m long model, D19, originally proposed for the SSC[2] . So far, results from the LHC program show that the use of NbTi is adequate for a field in the 9 tesla range in long magnets (10-15 m) that operate with superfluid helium at 1.8 K. Concerning the cooling, it must be mentioned that use of HeII has proven to be less complicated than expected; the increase in cost of superfluid helium with respect the normal LHe at 4.2 K is not dramatic, nevertheless it amounts to about 8-10% of the total cost of the cryomagnetic system (which for the LHC is about 100 MSFr) [3]

As far as Nb_3Sn is concerned, after pioneering work carried out at BNL about ten years ago, where different techniques have been tried on a 3 m long Nb_3Sn dipole that reached 8.5 tesla at 4.2 K [4] , the most important step in Europe was the CERN-ELIN collaboration on a 1 m long dipole, wound with conductor produced by VAC (D), that reached 9.5 tesla at 4.2 K [5] . The results could have been even better considering the fact that a field of 10.2 T was reached in a model where half coil and half iron, the so called "mirror dipole", where used: it was the first dipole winding breaking the 10 tesla barrier and still the record field at 4.2 K.

A few years ago two projects started, still underway, both aimed to build a 1 m long dipole with coils wound with Nb_3Sn cable in free bore of 50 mm:

- the LBL project, where 4 layers are employed to generate 13 tesla in a 50 mm coil aperture, D20 model dipole, [6] . This project was delayed with respect to the original plan, reflecting the technical challenge of such a magnet, anyway at the present time the complete Nb_3Sn coils are almost ready. Recently an intermediate step has been taken where the inner NbTi layer of the the above mentioned D19 dipole will be replaced with Nb_3Sn coils of similar current density as D20. This new step can proceed rapidly and can produce significant results within this year [7] .

  In the D20 project the problem of cabling Nb_3Sn wires has been deeply investigated by means of a high tech cabling facility of LBL. The Nb_3Sn wire are provided by TWCA (Albany, Oregon), whose material, produced according to the Jelly Roll Technique (a variant of the internal tin diffusion technique) has today the best J_c performance. Keystoned cables made of these vires have shown a high I_c degradation (10-20 %). For this reason a flat cable and a many wedges design have been adopted.

- the Univ. of Twente dipole, where 2 layers coils were arranged to generate 11.5 tesla in a 50 mm coil aperture with 17.7 kA current at 4.2 K, [8] (it started as a

twin dipole model, in the frame of the CERN-Twente collaboration for the LHC R&D). Many related studies have been carried out since the start of the project in 1989 (J_c vs strain, J_c vs compressive stress, thermal conductivity, insulation, etc.). The magnet was successfully tested in June 1995 at CERN. It reached 11.1 tesla with 18.7 kA at 4.2 K at the first quench, and the same field at the second quench. This value is the I_c limit which occurs on the splice between the conductors of the two layers. The field is few percent less than the one expected according to the initial design because they changed from a two apertures to a single aperture layout, and because the yoke saturation has been found more severe than calculated. A cable produced by a European company has been used: the PIT (Powder In Tube) Nb_3Sn by ECN (NL), at that time the Nb_3Sn with the best I_c ($J_c = 2000$ A/mm^2 at 10 tesla and 4.2 K). Few years ago ECN quitted the superconductivity business.

2.2 Quadrupole Magnets

The quadrupole of the LHC machine lattice are designed to generate a gradient of 220 T/m in a –twin– coil aperture of 56 mm, with NbTi conductor at 1.8 K.

For the *low* β inner triplet CERN has designed a special quadrupole [9] : it should generate a gradient of 250 T/m in a single aperture of 70 mm at 1.8 K, with a peak field on the coils of about 10 tesla. The magnet has many special features, described in a dedicated section and has been taken as reference in the present work [10] . The CERN basic design has been engineered by Oxford Instruments in a frame of a CERN-Oxford Ins. agreement, and a 1 m long model has been built and tested. at 4.2 K, reaching a short sample limit of 195 T/m. Test in superfluid helium are expected by June '95. Design, engineering, construction (test facility with 1.8 K refrigerator included) and testing took about three years.

A Nb_3Sn quad was built by CERN many years ago. The learned experience was a useful background for the construction of the above mentioned CERN-ELIN dipole.

The proposed quad has a peak field in the coil of about 12 tesla. This project can be a significant step in advancing Nb_3Sn magnet technology for quadrupoles as well as for dipoles. Moreover it addresses problems typical to quads, like the multiple connections of the coils and the required high field accuracy.

3 PROBLEMS RELATED TO THE USE OF Nb_3Sn

It is well known that Nb_3Sn has two main drawbacks:

1. Technical difficulty

   - the conductor needs to be reacted at temperature around 650-700 °C for long time (two weeks) to allow tin to diffuse into niobium filaments to form the Nb_3Sn compounds

   - Nb_3Sn is very brittle and a maximum strain of 0.25-0.3% is allowed before J_c starts to degrade. Actually degradation starts at strain around 0.5-0.6% but uncertainty in determining the exact stress distribution in the coils, limits the acceptable strain in the design at half of the nominal value.

This two characteristics oblige first to Wind the coil and then to React it at a high temperature, called *W & R* technique (the other technique, *R & W* , being forbidden in accelerator magnets by the high strain, typically 2-5%, induced by the small curvature radius at the coil ends). With *W & R* the winding is easy, at least not more difficult than NbTi, but the insulation must withstand such high temperature. Glass tape or braid is usually a good solution but glass has two disadvantages: 1) it's thicker than the Kapton tape (the insulation used in the CERN-Oxford quad) and mechanically weaker, 2) the glass always comes impregnated with a binder, that must be taken off before the thermal treatment otherwise it develops carbon with loss of insulation and severe danger in case of quench. To get rid of the binder (or sizing agent) without damaging the Nb_3Sn wire is usually a prominent part of the job.

The brittleness after heat treatment makes it almost mandatory to impregnate the coil with resin. Impregnation decreases the coil stability against mechanical or thermal disturbances because the cooling is indirect but it has also the beneficial effect to reduce movements of single strands or of the whole cable.

Because of the Nb_3Sn brittleness some concern can be raised on the maximum reasonable length of the coils: while it is clear that 15 m long coils in Nb_3Sn may be too difficult to handle, we believe that 5 m long coils, like the ones needed for the LHC *low β* quads, are not unrealistic considering that 3 m long coils have been successfully built at BNL few years ago.

2. Cost higher than NbTi. Cost analysis can be broken into subitems:

    *   the cost of the conductor. Usually Nb_3Sn costs more than twice than NbTi. Europa Metalli (Florence) is now marketing a Nb_3Sn wire whose cost is comparable with that of NbTi wire of the LHC pre-series dipole model and prototype (1989-94). This is due to improvements production technique, the so called Internal Tin Diffusion, ITD, that is by far less expensive and faster than the Bronze Route technique (in which Vacuumschmelze is still unsurpassed and that gives the better quality –filament diameter of 3 μm – but that yields J_c 40% lower than ITD).

    *   the cost of the coil manufacture. This cost can be again split into two parts: 1) cost of the tooling, i.e. oven of high homogeneity at 700 °C and impregnation tools, 2) cost of reacting the coil, of moulding operation and extra-time needed for handling the coil with extreme care. Skipping point 1 (tooling depends on facilities available in the construction site and tends to be negligible if a number of magnets are to be built) the increase of the cost associated with manufacture Nb_3Sn coils instead of NbTi coils is approximately 30% (this figure is inclusive also of the risk associated with coil handling).

Because the cost of the coil manufacture is typically 30% of the total cost of a superconducting magnet, the total increase of cost for a finished accelerator magnet is "only" 10% higher for Nb_3Sn than for NbTi, if the mechanical structure (collaring, yoking, shrinking cylinder) is to be the same. Of course higher field asks for stronger (and expensive) mechanical structure but this is just the fee for better performances and should not enter in the comparison.
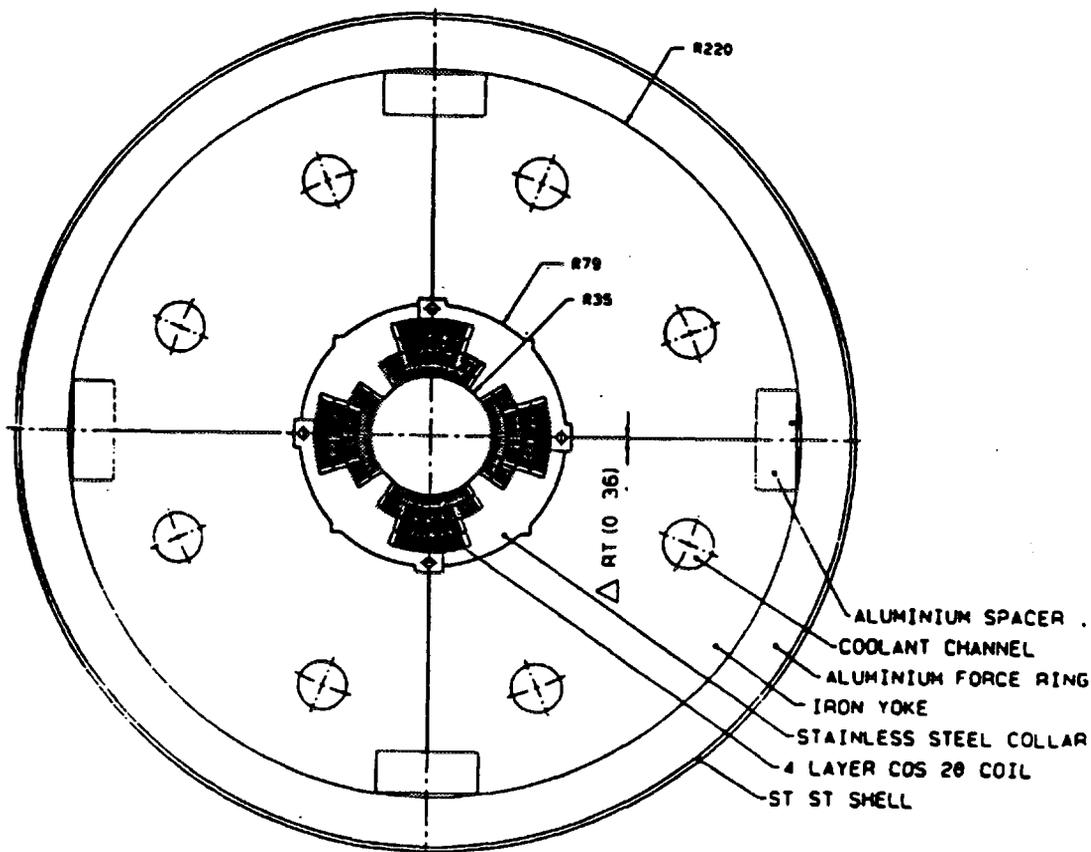
FIG. 3: cross section of the CERN-Oxford Ins. quadrupole (CERN courtesy).

It should be mentioned that the tooling cost can be significant in constructing the first model and/or prototype and that the cost associated with R&D is not negligible.

4 REFERENCE DESIGN AND SCALING LAWS

4.1 The CERN-Oxford Quadrupole

The quad, mentioned in the panorama as a milestone, is designed for a gradient of 250 T/m at 1.8 K in a single aperture of 70 mm[10] .

The magnet, whose cross section is shown in fig. 3, has windings with very high performance NbTi conductor: J_c is 10-15% higher than in the cable for the LHC dipole (having a filament diameter of 10 μm while for the dipole conductor is 6-7 μm). Furthermore the α (α=Cu/non Cu) is small, 1.3 while is 1.6–1.9 in the cable for dipoles, and the cable insulation is extremely thin: 75 μm per side, against 120 μm per side for our dipoles. Such a thin insulation has been obtained by use of special Kapton, developed for the SSC project.

The three mentioned characteristics (J_c, α and insulation thickness) increase the average current density to the outstanding values of 440 A/mm^{2}at 9.65 tesla and 1.8 K for the layers shells and of 640 A/mm^{2}at 8.23 T for the outer layers.

The coil features, as shown in fig. 3, can be summarized as:

- use of four layers windings, result in a low operating current ($\leq$ 5000 A). Four layers are not commonly used and to our knowledge is the first superconducting quadrupole with this feature.

- special grading of the current density: usually the grading is done using a cable with smaller dimensions in the outer shells, like in the main LHC dipoles, where the field is low and the superconductor has higher J_c. In case of 4 shells it is customary to use a smaller cable –with the same current– in the two outer shells. Here the smaller cable is used also inside the second shell, in a low field region from midplane up to 2/3 of the shell height, thus increasing the total turn numbers. As a consequence a splice inside the layer is required between the small cable and the big one.

- the use of a cable with an ideal keystone angle –which means that the insulated cable is a perfect radial sector– avoids the need of longitudinal spacers, thus increasing the total filling factor. The ideal keystone angle has been obtained without substantial J_c degradation.

Of course such a design, which is really optimized for the the given aperture and material, is not without problem: the inductance is high and protection becomes more difficult especially for the full length magnet. The special grading of the second shell requires a joint between the two cables inside a shell, which increases complexity and cost.

4.2   Coil Design

A preliminary decision was made to eliminate any joint between cables (splice) inside the winding (required by the special grading): it would not be compatible with the Nb_3Sn heat treatment. A basic feature is also to wind the layers in double pancake technique. This imply that layers are either two or four (more would be not practical). The use of a double pancake winding technique has two major benefits:

1. reduction of the number of splices inside the coils: only one splice for a 4 layer magnet or no splice at all for two layers;

2. whatever the layer number, all electrical connections are out of the coil volume, in a very low field region, and well cooled. Experience on the dipole models and prototypes, have shown that the splice inside the coil is usually a weak point.

3. elimination of the splice in the winding is a gain in time construction and cost.

4.2.1   Coil Shape: Circular Shells vs Rectangular Blocks

An extensive investigation has been carried out comparing magnetic efficiency of coil wound in circular "cos θ" shell and rectangular coil block. The idea of rectangular coil block has been advanced in the past for dipoles and recently investigated by CERN [11] . Analytical code based on complex variables has been developed for the calculation of the field, gradient and multipole expansion coefficients in the coil-free region as well as computation of the peak field on the coil both for circular shells and rectangular

blocks. Analytical formulae for the multipoles of rectangular blocks have been derived, [12] , since to our knowledge no publication has been made on the subject.

The code can include contributions from a circular iron yoke. Permeability can have any –constant– value. The whole mathematical treatment and code description is under publication [13] .

The main modification of the CERN-Oxford design was elimination of the special grading of the second shell (as previously mentioned it does not fit Nb_3Sn technology); with circular shells the gradient of the reference design is 241 T/m vs the 250 T/m of the actual CERN-Oxford quad.

Taking a simplified version of the CERN-Oxford quad as reference, we also designed the "corresponding" quad built with rectangular coils, giving 224 T/m.

In the fig. 4 a sketch of the cross sections (only an octant) of the two quads is shown. Main features are:

1. coils are wound in four layers with the same NbTi cable of the CERN-Oxford, with a layer thickness of 8.3 mm;

2. the grading ratio, i.e. $J_2/J_1 = 1.44$, where J_1 is the overall current density of the two inner coil shells (the ones where the field is high) and J_2 is the current density in the two outer, low field, shell. In the rectangular coils the grading ratio has been changed into 1.52 in order to have the same efficiency in all coil blocks;

3. since there is no special grading in the second shell, basically the four layers are equivalent to two big layers, both for circular and rectangular coils. The height ratio is optimized to minimize the multipole content;

4. iron permeability was fixed at $\mu_r = 6$ because this is the equivalent μ_r for the CERN-Oxford. The iron yoke is circular also for the rectangular coil quad.

5. the rectangular blocks have a gap between the coil and the midplane. The (half)gap is 2 mm for 70 mm coil aperture. This gap gives a 7% penalty on the gradient but is necessary for rectangular blocks to have a reasonable minimization of the multipole content (especially b_6, by far the most dangerous). While the circular coil can avoid this penalty, it is possible that a gap will be required to avoid coil heating by secondary radiation form collision point.

Comparison between the two coil shape is summarized in table 3. Lack of special grading in the second shell results in 4% less gradient for both design. The rectangular block quad gives 224 T/m of field gradient, 7% less than the circular one (241 T/m): this penalty reduces to 3-4% if a midplane gap is introduced also in the circular shell design.

4.2.2 Scaling Laws

After this first comparison the results where scaled for different coil apertures and gradients. The scaling is plotted in a plane where the coordinates are the peak field of the coil and the overall current density in the inner coils. The overall critical current density curves of a NbTi cable at 1.8 K and a Nb_3Sn one at 4.2 K and 1.8 K are also plotted in order to show the feasibility of each design.

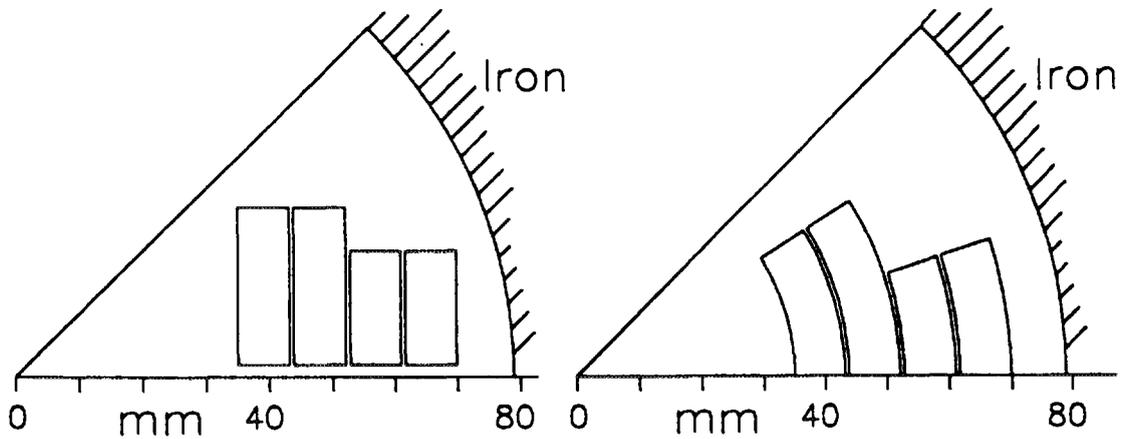Before examining the result of the scaling it should be noted that:

FIG. 4: sketch of the two reference quadrupoles (only one octant cross section): to the right the circular shell coils (basically the CERN-Oxford quad without special grading), to the left the "corresponding" rectangular block coils.

- the grading ratio, J_2/J_1, is kept constant: 1.44 for circular shells and 1.52 for rectangular blocks, the values of reference design. As a consequence of this restriction the abscissa is representative of the current density of the whole coil.

- geometrical dimension are scaled linearly with coil aperture. This imply that coil height is kept at constant angle and a fully keystoned cable.

- along the iso-gradient contour lines the peak field on the coil increase linearly with the coil aperture, nevertheless it is worthwhile to remark that the peak field is substantially higher (more than 10%) than $B_{max}=$Radius$\times$Gradient, valid for an ideal quadrupole.

- NbTi and Nb$_3$Sn characteristics are in terms of overall critical current density of a winding (copper, insulation and cabling filling factor and degradation are already included).

Results obtained by the scaling are shown in fig. 5 for circular shells and for rectangular blocks. It can be noted that the advantage of Nb$_3$Sn at 4.2 K with respect to NbTi at 1.8 K tends to vanish if very high current density have to be used, i.e. for very high gradient and "small" coil aperture, while Nb$_3$Sn shows the best advantage when large coil aperture are required. It is possible that the outer quad of the *low* β inner triplet will be required to have a coil diameter of 100 mm [14] and in this case a gradient of 200 T/m with Nb$_3$Sn cable can be reached at 4.2 K and even 225 T/m at 1.8 K with a very comfortable margin in case of circular coils and a small margin with rectangular coils.

Moving from the starting points, in examining the fig. 5, we see that a small gain can be made by Nb$_3$Sn at 4.2 K. An appreciable gain over NbTi at 1.8 K is given by Nb$_3$Sn only at 1.8 K, consequently in the following the two materials will be compared always at the same temperature of 1.8 K. We remember also that any value is given at 93% of the crossing of the B=B(J) load line and the B=B(J) critical current line, i.e. we keep a 7% margin of the operating current to the short sample critical current.

Moving along the constant aperture line $\phi= 70$ mm we see that with circular coil surrounded by iron the maximum gradient with Nb$_3$Sn is almost 300 T/m. In principle

TABLE 3: Parameters of the two reference designs used for scaling. Lengths are in mm, angles in degrees. X,Y refers to rectangular shape and R to circular shells, see fig.5.

	rect.	shell
int.radius coil 1 (X_1,R_1)	35	35
ext.radius coil 1 (X_2,R_2)	43.2	43.2
int.radius coil 2	43.9	43.9
ext.radius coil 2	52.1	52.1
int.radius coil 3	52.8	52.8
ext.radius coil 3	61	61
int.radius coil 4	61.7	61.7
ext.radius coil 4	69.9	69.9
half height coil 1,2 (Y_2)	27	
half height coil 3,4	20	
half height shim 1,2,3,4 (Y_1)	2	
half angle coil 1,2 (β)		32.2
half angle coil 3,4		18
half angle shim 1,2,3,4 (α)		0
iron radius (R_{iron})	79	79
iron permeability	6	6
B2 (T at 1 cm)	2.24	2.41
B6 (T at 1 cm)	$-6.0\ 10^{-6}$	$2.8\ 10^{-6}$
B10 (T at 1 cm)	$-2.5\ 10^{-6}$	$-2.4\ 10^{-6}$
J_1 (A/mm^2)	460	460
J_2 (A/mm^2)	700	660
B_{max} cable 1 (T)	9.57	9.51
B_{max} cable 2 (T)	7.48	8.19
J_1/J_{max}	93 %	93 %
J_2/J_{max}	89 %	89 %
NI (kA/octant)	395	393

this 50 T/m more gradient given by Nb_3Sn only requires a slightly bigger yoke (full saturation is to be avoided) and an operating current 20% higher.

Moving along the iso-gradient line of G = 250 T/m (the nominal gradient of the CERN-Oxford Instruments model) we see that Nb_3Sn can allow an aperture of about 90 mm, again with circular coils with iron yoke. That means that moving around the reference points a 20% margin either in aperture or in gradient strength is permitted.

As far as rectangular coils are concerned, the scaling shows a behaviour similar to the previous one, the difference owed to the supposed less degradation of Nb_3Sn due to the fact that with rectangular coils a flat cable instead of a trapezoidal one is needed. In this study, based on our previous experience on flat cable and experience of LBL on trapezoidal cable, we keep 5% I_c degradation for flat cable and 10% for keystoned cable. This increases slightly the gap between Nb_3Sn and NbTi J_c curves. With a rectangular coil configuration (fig. 5), it is possible to generate, again at 93% of the maximum nominal current, a gradient of 280 T/m in a ϕ=70 mm coil aperture or equivalently to have a coil aperture of 82 mm with gradient of 250 T/m. These
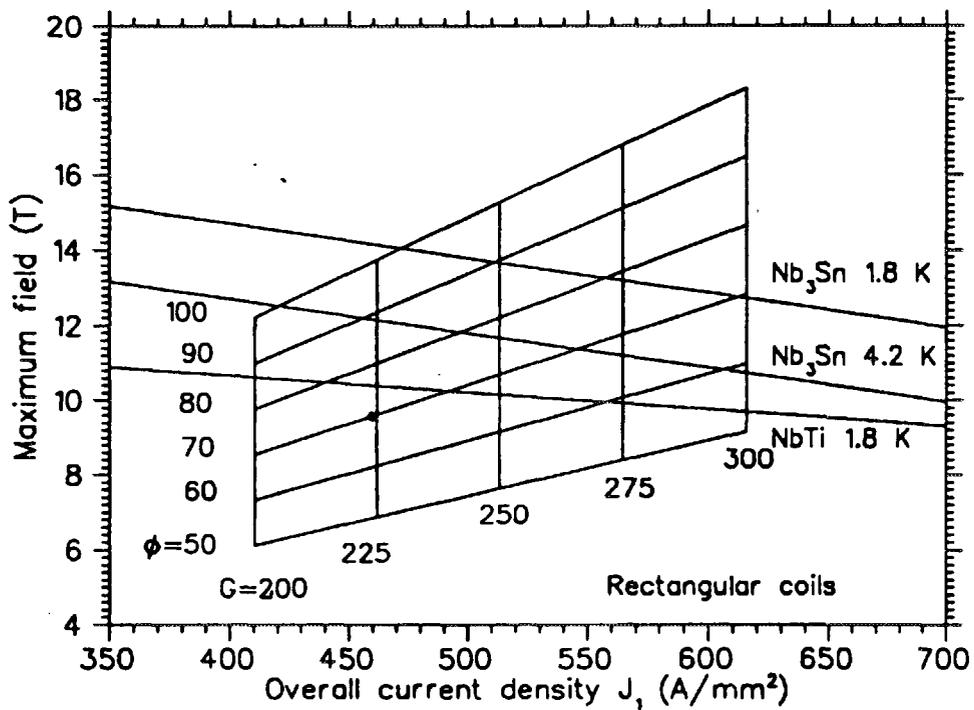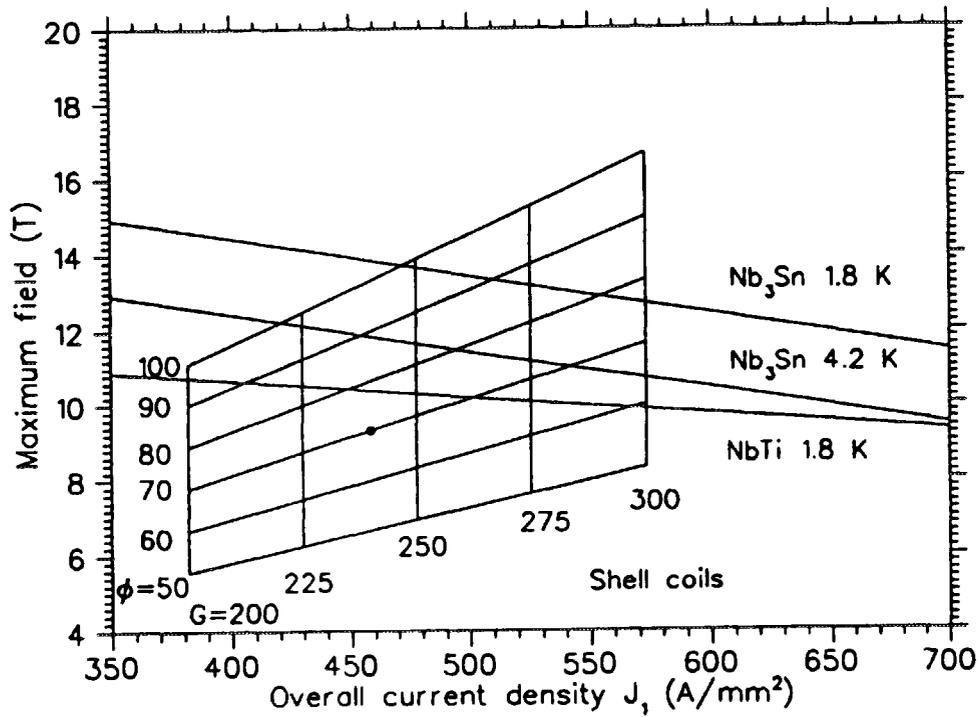
FIG. 5: scaling diagrams for circular shells (top) and for rectangular blocks. Overall J_c for NbTi and Nb$_3$Sn windings are reported, too. Coil aperture ϕ in mm; gradient G in T/m. Dots indicate the reference designs position.

figures are well above the reference designs, both the circular and the rectangular coils, indicated with dots in fig. 5. They are 15% higher than the optimized best design of the NbTi CERN-Oxford quadrupole: nevertheless they are about 7 % less than the

corresponding figures given by the circular shell quad (remembering that a 2 mm half gap is required between the midplane and the coils in the rectangular design).

Examining the diagrams obtained for iron free quadrupoles (fig. 6), for shell coils and for rectangular coils, one notes that the allowable gradient-aperture combinations are surprisingly near the yoked quadrupole, the penalty for missing the iron yoke being only 2-3%. Actually the iron contribution to the gradient is small when compared with the coil contribution but not negligible: around 15%. This contribution appears also as field on the coil, increasing significantly the peak field. When iron is missing the peak field decreases and the 15% loss in gradient can be partially regained by increasing the current density in the coils (about 12-13%).

4.2.3 Choice of Yoked Circular Coils

Many routes are open in order to test the better performance allowed by Nb_3Sn conductors. First we decided to drop the option for a rectangular cross-section. At the beginning this option seemed to be advantageous in view of the various possible benefits:

- easiness in winding;

- improved precision in the coil stack dimension (one should not forget that these quadrupole must have final accuracy at least five times better than the machine quadrupole);

- easier way to control the e.m. forces, which are unusually high for a quadrupole.

Regarding the first point, after discussions with an experienced magnet builder company, it was found not to be valid. The rectangular shape for a quadrupole can raise serious problems at the coil ends because of the narrow bend of the inner turn (the one near the 45°line of the quadrant). Experience with large dipoles for LHC have shown also that the accuracy of shell-like coils can be as high as desired – in principle – being determined only by the accuracy of the winding mandrel and handling accuracy. If anything is properly done, the accuracy is eventually determined by cable plus insulation tolerances. It is not so clear that flat surfaces can be effectively machined with better accuracy than curved ones. With respect to the forces a rectangular shape may have some advantage, but not so important as to polarize the choice. At this point we think it is better to proceed with a design based on circular shell coils: it gives a 7% gain in the gradient over the rectangular shape, and seems easier to be built. Even in case a shim is required in the midplane also for circular coils they give at least 4% gradient more than rectangular block coils.

As far as the iron yoke we think that it's worthwhile to keep it. It has the following advantages over the iron free equivalent version:

1. 3% more gradient;

2. 12% less current. This means a 20% reduction in power dissipation during a quench, which is relevant for the magnet protection;

3. a magnet flux shield is always recommended; stray field is not a key point, anyway it is not negligible and may be required in real quadrupole placed in the tunnel.
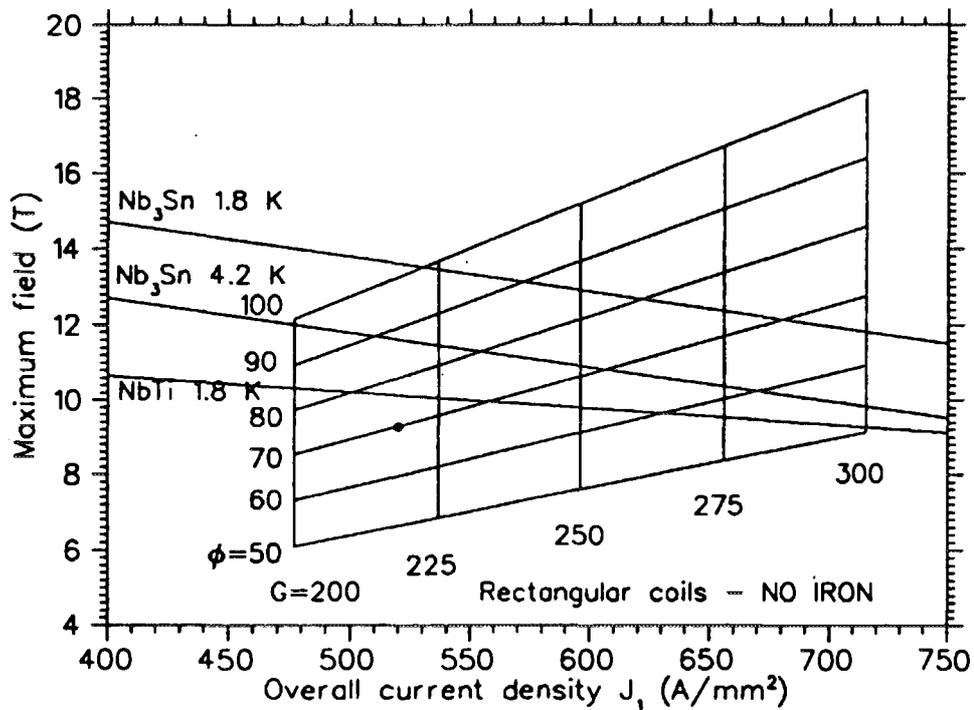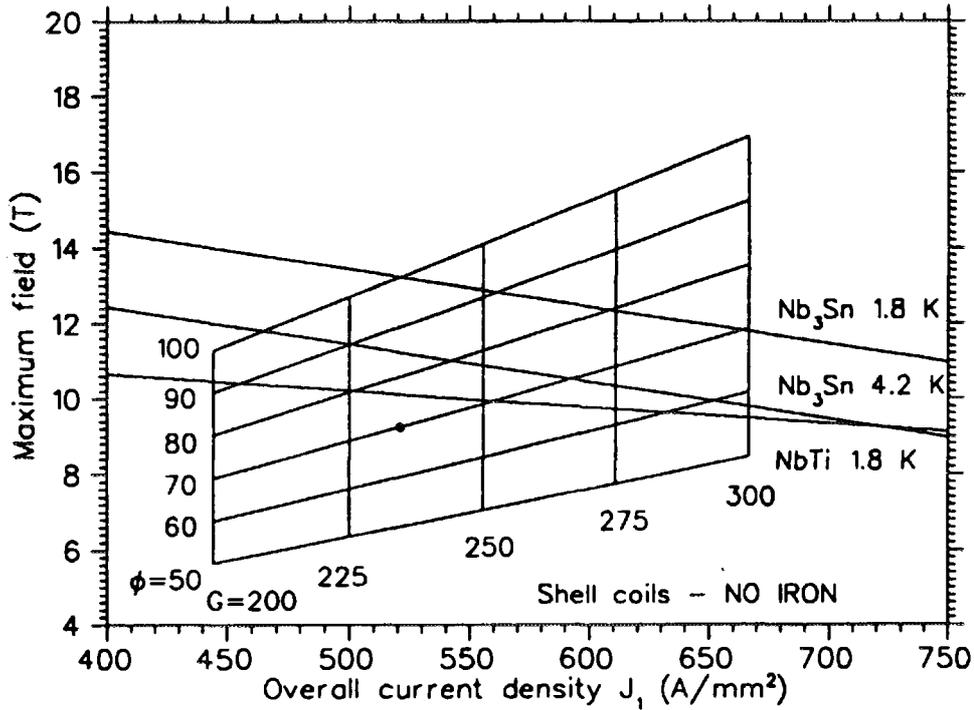
FIG. 6: scaling diagram for circular shells (top) and for rectangular blocks (bottom) without Fe-yoke. Overall J_c for NbTi and Nb3Sn windings are reported, too. Coil aperture ϕ in mm; gradient G in T/m. Dots indicate the reference designs position.

Because the contribution of the iron is desired but not critical, we feel it is not extremely important to place the iron so near to the coil. It's hard to loose more than 1% of the gradient even if the yoke is far away, let's say 40 mm instead of 8 mm like in the

CERN-Oxford design. This means that in our case the iron is merely a flux return yoke and this feature will have important consequence for the mechanical design.

It is possible that the inner quadrupole of the triplet will be required to have a small aperture, a high gradient and to be *iron free* [14] since it is exposed to the detector's field and because it will be cantilevered (and weigh can be an issue), it is worthy to note that more than 350 T/m can be generated in a 50 mm coil aperture using Nb_3Sn at 1.8 K.

The magnet configuration is based on *circular coils surrounded by iron yoke*. As already mentioned in the previous subsection, we can put the benefit of Nb_3Sn either on higher gradients or on larger apertures (or as a partial gain for both). We decided to have a larger aperture because it makes the best use of Nb_3Sn material. Also the stability against radiation will be helped by this increment of radius, reducing the number of particles that will hit the coils. Large aperture will make it also easier to wind improving the winding accuracy for the chosen cable that is rather big, especially at the coil ends.

From the point of view of the machine performance a higher gradient would have been more welcomed: in case of different CERN preference (more gradient with the same aperture) our choice can be changed. Nevertheless one should not forget that the 20% larger bore means a net gain in accuracy and a reduction in the alignment accuracy [14].

5 DESCRIPTION OF THE PROPOSED QUADRUPOLE

5.1 Choice of the Conductor

The J_c vs field characteristics of the best NbTi (the one used for the CERN-Oxford quad) and of Nb_3Sn are reported in fig. 7 together with the actual average current density of the coils, i.e. the J_c scaled down by copper fraction, by cable filling factor, by cabling degradation (3% for NbTi and a prudential 10% for Nb_3Sn) and by the insulation filling factor. The curves show that the threshold for use of Nb_3Sn is when the peak field in the conductor is larger than 10 T.

Nb_3Sn can have a small copper fraction; $\alpha=1.1$ for our Nb_3Sn cable (and can be lowered to values of 0.8–1 if needed), however this will be a disadvantage for the protection of the magnet (as discussed in the dedicated subsection).

The shape of the cable has been chosen equal to the outer cable of the LHC dipole: 36 strands with $\phi= 0.825$ mm to give a cable with 1.47 mm of average thickness $\times 15$ mm of width. The keystone angle is 1.0° , wider angles were excluded because strong degradation may be expected and it will need an appropriate R&D program to test the cables.

The shape of the conductor was frozen following these considerations:

- all the tooling exits in EM-LMI (or in any other company working for the LHC project) for such a shape. Different shape means new tooling and more time to set the cabling line. We think it is not worthwhile in this phase of the program;

- while smaller strands and less number of strand to compose the cable could be beneficial because would mean thinner cable with better flexibility and possibly less conductor volume for the same gradient, our choice tends to minimize the
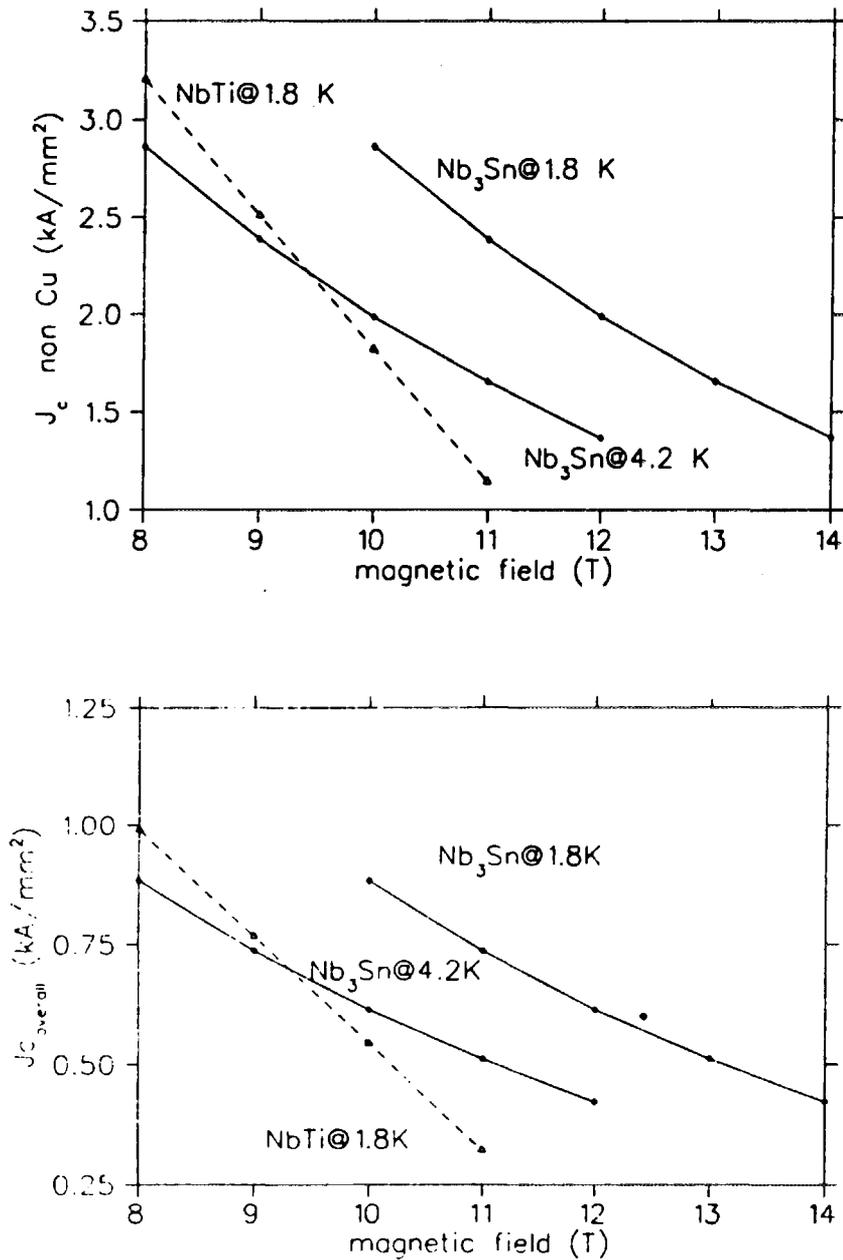
FIG. 7: top: non copper J_c vs field characteristics of the best NbTi (produced by Outokumpu - F, courtesy of Oxford Ins.) and of Nb₃Sn produced by Europa Metalli; bottom: overall J_c for the same conductor, see text for details

insulation cross section and the coils inductance, that is important for magnet protection.

A preliminary piece length of 100 m of Nb₃Sn Rutherford cable has been produced by EM-LMI: the measured J_c values are just the ones reported in fig. 7 (measured at 4.2 K, calculated with a 2 T shift at 1.8 K).

TABLE 4: main features of different variants for a circular Nb_3Sn coil yoked quadrupole. Coil aperture is 85 mm. Gd is the grading ratio, J_{out}/J_{in}.

Model (shells)	cable (mm)	Iron yoke	Grad. (T/m)	Temp. (K)	I oper. (kA)	$J_{over.}$ (A/mm^2)	B peak (T)
4 Nb_3Sn	15	yes	241	4.2			
3 Nb_3Sn	15	yes	231	4.2	10.4	390	11.4
2 Nb_3Sn	15	yes	214	4.2	13.1	490	10.4
1Nb_3Sn +1NbTi	15	yes	185	4.2	16.6	620	9.0
2Nb_3Sn +2NbTi	15	yes	223	4.2	11.6	434	10.9
Cern-Oxf.	10	yes	261	1.8	8.24	463	12.5
4Nb_3Sn Gd=1.44	10	yes	254	1.8	8.24	463	12.5
4Nb_3Sn Gd=1.13	10	yes	253	1.8	8.29	466	12.5
4Nb_3Sn Gd=1.13	15	yes	265	1.8	10.2	380	13.3
4 Nb_3Sn	15	yes	264	1.8	10.5	390	13.2
2Nb_3Sn +2Nb_3Sn	15	yes	257	1.8	12.2	455	12.6
3 Nb_3Sn	15	yes	257	1.8	11.8	441	12.7
2 Nb_3Sn	15	yes	241	1.8	14.6	546	11.7
4Nb_3Sn Gd=1.13	15	no	259	1.8	11.1	415	13.0
4 Nb_3Sn	15	no	259	1.8	11.6	435	12.8
2Nb_3Sn +2Nb_3Sn	15	no	251	1.8	13.1	490	12.2
3 Nb_3Sn	15	no	249	1.8	13.2	495	12.2
2 Nb_3Sn	15	no	225	1.8	16.4	615	11.0

5.2 Coil Layouts

In table 4 are reported the main results of the investigation carried out to select the best coil layout. We note that because of the large number of explored design, the different layouts are far from optimization.

Insulation was selected to be glass tape with an average thickness on each side of 125 μm and 250 μm of radial insulation. On the midplane a further insulation 0.3 mm thick is placed to improve both inter-coil insulation and to leave some channel for HeII cooling.

While most cases are with the 15 mm wide cable, the chosen one, few cases computed with a smaller 10 mm cable are reported for comparison. The gain in passing from 10 mm wide to 15 mm wide cable is small, 12 T/m in term of gradient. Nevertheless this gain is magnified by the decrease of 20% of the current density, which makes the magnet much more stable and safe against a quench. The grading of the current density turned out not so efficient with the Nb_3Sn cable size we have examined so far.

Three coil designs have been selected and explored with the real conductor also using the code ROXIE developed at CERN [15].

With respect to the scaling law applied to the reference design, presented in the previous section, and to the results of table 4, we have to point out that:

• the conductor has not perfect keystone angle, at least for the inner shell. Longitudinal copper spacers, or coil wedges, have to be inserted to regain circularity or to adjust the layer height for multipole compensation, with consequent reduction of the gradient;
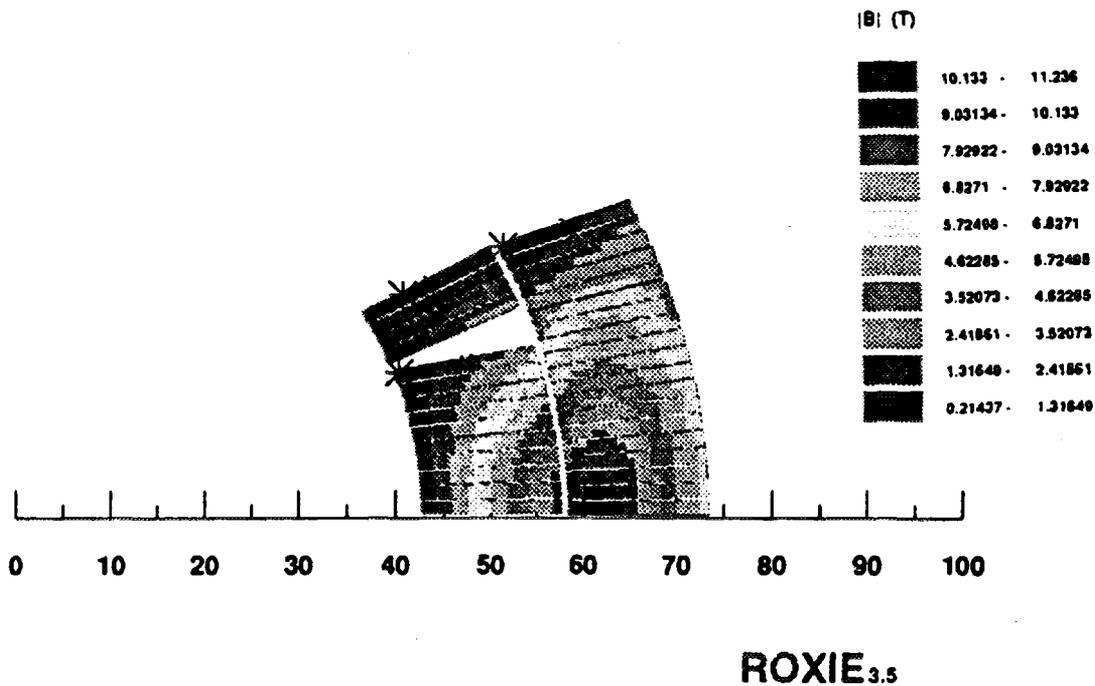
|B| (T)

�	10.133 · 11.236
▰	9.03134 · 10.133
▰	7.92922 · 9.03134
▒	6.8271 · 7.92922
░	5.72408 · 6.8271
▒	4.62285 · 5.72408
▰	3.52073 · 4.62285
▰	2.41861 · 3.52073
▰	1.31649 · 2.41861
▰	0.21437 · 1.31649

0   10   20   30   40   50   60   70   80   90   100

ROXIE₃.₅

FIG. 8: two shells Nb₃Sn quad: coil cross section (only an octant) with field contour lines

- grading, that is intrinsically less for Nb₃Sn than for NbTi, has not been considered;

- the cable size was not exactly scaled with respect to the reference design.

All this together means that designs can be further optimized with proper selection of cable sizes for each layer.

The three designs have been investigated and compared also for the stress analysis and magnet protection.

5.2.1   2S – two shells layout: 85 mm, 241 T/m

The coil cross section is shown in fig. 8. It consists of a single double pancake coil per quadrant and it is basically the reference design, see subsection on scaling law, where two by two the layer are unified, having used a 15 mm wide cable instead of the 8.3 mm wide NbTi cable of the CERN-Oxford quad.

This magnet does not have real problem from the structural point of view: stress in the coil is large but within the explored capability of Nb₃Sn and also construction is more simple than the other alternatives. There is no splice but only joints between poles. Protection is not easy, the current density is very high, $J_{overall}$ around 550 A/mm² but the inductance is not very large and this cope to dump the current. The big operating current, around 15 kA, is surely one of the few drawbacks of this choice. Magnetic forces on coils are: $F_x = 163.5$ ton/m, $F_y = -230$ ton/m ($F_r = 75.7$ ton/m, $F_{theta} = -266$ ton/m).
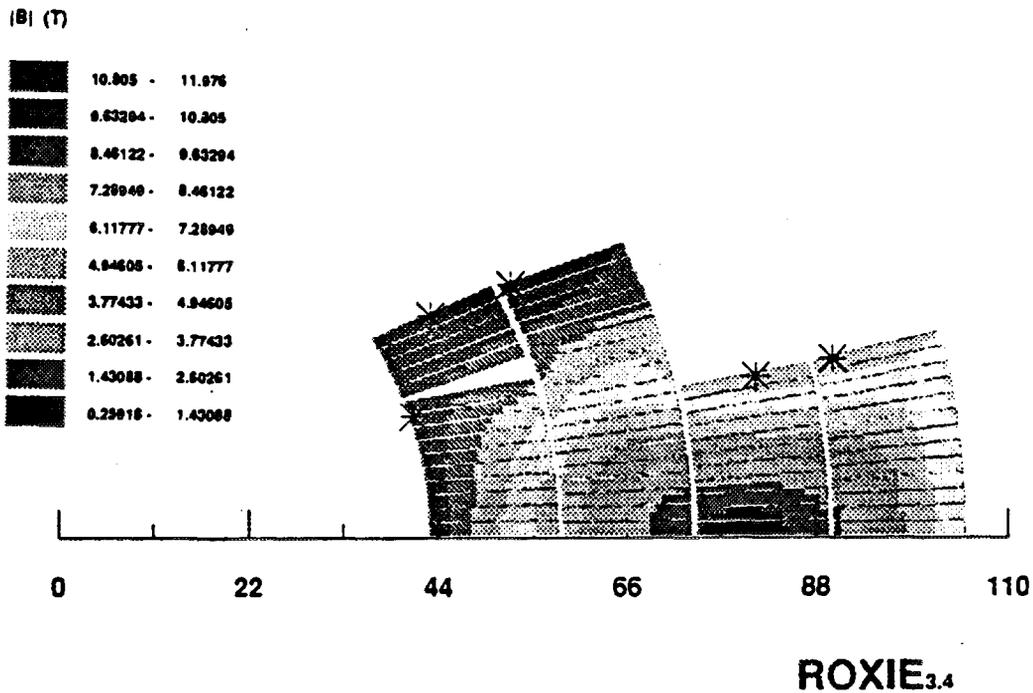
|B| (T)

■	10.505 -	11.076
■	9.63204 -	10.505
■	8.46122 -	9.63204
▓	7.28040 -	8.46122
░	6.11777 -	7.28040
▓	4.94605 -	6.11777
▓	3.77433 -	4.94605
▓	2.60261 -	3.77433
■	1.43088 -	2.60261
■	0.25916 -	1.43088

0   22   44   66   88   110

ROXIE₃.₄

FIG. 9: two plus two shells Nb₃Sn quad: coil cross section (only an octant) with field contour lines

5.2.2 2S+2S – two plus two shells layout: 85 mm, 258 T/m

Higher gradient is given by the a four layers coil design, which we call two plus two. Two wide (in azimuthal extension) shells form the first double pancake, while two additional shells with a smaller azimuthal extension form the second double pancake. In fig. 9 a cross section of this coil design is shown.

The outer double pancake can be wound either with NbTi cable or with Nb₃Sn cable. The achievable gradient is not really different, the only advantage of Nb₃Sn over NbTi being the much higher I_c (the limit is of course on the inner double pancake) and the fact that only one technique (although the difficult one) is used in the whole coil construction. The gradient, in the 85 mm coil aperture is 258 T/m, with a comfortable reduction – with respect to the two shells design – of the current density from 546 to 455 A/mm². This beneficial effect, lower power dissipation, largely balances the increase of inductance which otherwise would have been a serious drawback in the protection. Magnetic forces on coils for a magnet without yoke are: $F_x = 177.3$ ton/m, $F_y = -337.6$ ton/m ($F_r = 74.7$ ton/m, $F_{theta} = -381$ ton/m).

5.2.3 4S – four shells layout: 85 mm, 264 T/m

If the outer double pancake, i.e. the two outer shells, are wound with Nb₃Sn conductor, all layers can have the same azimuthal extension, still being the inner two shell the limiting, at 93%, ones. This results surely in an increase in conductor costs and coil weight but yield two main advantages: a gradient 2% higher than the "two plus two" design and a lower overall current density: "only" 380 A/mm²making not too difficult the protection despite the bigger inductance. A cross section of this quadrupole design

|B| (T)

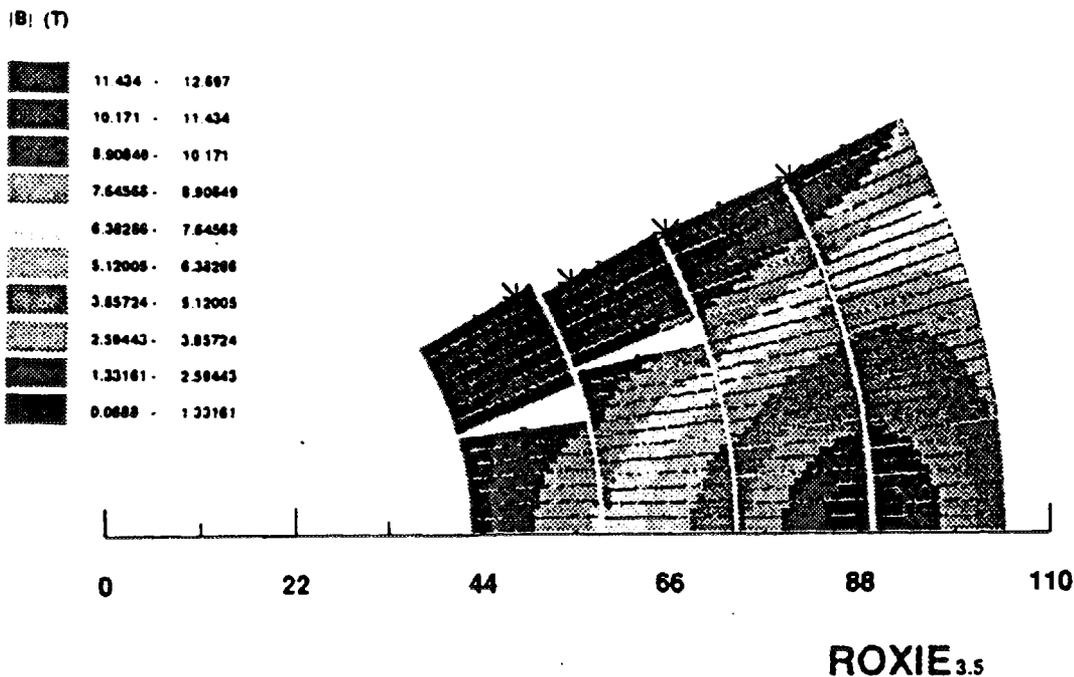|	
11.434 -	12.697
10.171 -	11.434
8.90848 -	10.171
7.64568 -	8.90849
6.38286 -	7.64568
5.12005 -	6.38296
3.85724 -	5.12005
2.59443 -	3.85724
1.33161 -	2.59443
0.0688 -	1.33161

0   22   44   66   88   110

ROXIE₃.₅

FIG. 10: four shells Nb₃Sn quad: coil cross section (only an octant) with field contour lines

is reported in fig. 10.

A disadvantage of this magnet is the heavy mechanical structure, the complexity of the stress application, the high stress in the coils at full current and the cross section that have the same size of the twin dipole cross section (an increased flux translates into a thicker yoke in order to avoid severe saturation effect). Magnetic forces on coils for a magnet without yoke are: $F_x = 226$ ton/m, $F_y = -397.9$ ton/m ($F_r = 82.5$ ton/m, $F_{theta} = -445.7$ ton/m).

5.3   Mechanical Design and Stress Analysis

Since the iron does not contribute significantly to the gradient –but allows to lower the current density and so helps the magnet protection– a considerable space is left between the coils and the yoke. In this way the collars can be thick and can be designed to support the whole e.m. forces. With this choice iron does not give contribution to the mechanical structure and is a mere flux return yoke.

This feature simplify the design and construction: the LHC main dipoles and the CERN-Oxford quadrupole both requires gap in the iron halves or quadrants, These gaps must be kept under strict control within 0.1 mm or better in order to assure a correct mechanical performance. In our case the yoke is simply assembled onto the collars, with a reasonable clearance, and helps only to avoid torsion of the magnet along the length. The outer stainless steel cylinder is basically the helium vessel and can be made as thin as 3 mm. No particular care is put on the outer cylinder welding because we don't need any prestress from the iron.

Since we rely only on the collars as mechanical containment of the e.m. forces, great care has been devote to the collar design and collaring concept. Different solutions have

been investigated:

- "traditional" collar, of adequate thickness made out of high strength aluminum alloy. The collars are arcs with a wedge attached, see for example in fig. 3 the collars of the CERN-Oxford quad.

- a design where the collar is split into a ring that works as a coil restraining cylinder, made out of the Al alloy, and a wedge between the coils (in the region where in the classical magnets was the iron pole). The wedge is supported by the outer ring but can be made out of a different material. The full section of the four shells magnet with this ring-wedge collar system is shown in fig. 11.

  The advantage of this solution is to get the maximum benefit from the different thermal contraction of the materials. In fact aluminum, and its alloys, contracts more than the coil, so during cool down the ring puts a radial pressure on the coil. On the other side the wedge, if made out of stainless steel (or, even better, of titanium alloy) contracts less than the coil stack, increasing the azimuthal stress in the coils In this way the collar assembly is more critical but prestress can be lowered.

  Another great advantage envisaged by this ring-wedge system in conjunction with the use of Ti alloy as material for wedge, is the fact that the wedge can be used as winding post thus avoiding coil handling. Advantageous is also the fact that axially the wedge will keep the coil in tension: we expect this feature to help in keeping very low the void fraction in the coil ends.

  Other new materials for the wedge, like high strength ceramics, will be explored as a low thermal contraction material for the wedge in a next development step.

The design of the collars is strictly connected with the collaring system. At present we have two solutions:

- pressing in one direction, like in a dipole, with one big press which may be available in few companies. In this case collars are split in two halves, much like in the dipole magnet. The difficulty of this solution is to apply the same prestress to all coils.

- pressing along two perpendicular axes, like a cross. In this way the quadrupole symmetry is respected and, if everything is well done, the pressure apply in the same way on all four coils and the movement of the collar-coil system during collaring operation is minimized. Indeed the center of magnet is kept fixed, thus the relative alignment of the coils along the nominal radius is easier with benefit in avoiding the unwanted multipole components which comes from coil misalignment. In this solutions the collars are subdivided in four quadrants.

While a solution has been found also with the case of the collars split into two halves, the subdivision in quadrants is preferred because in the first case an error in the dimensions or in assembly is not forgiven and results immediately in a coil dissymmetry.

In order to carry out the collaring by quadrants, we can use either a dipole press with a special arrangement (which looks possible but not at all easy) or a special
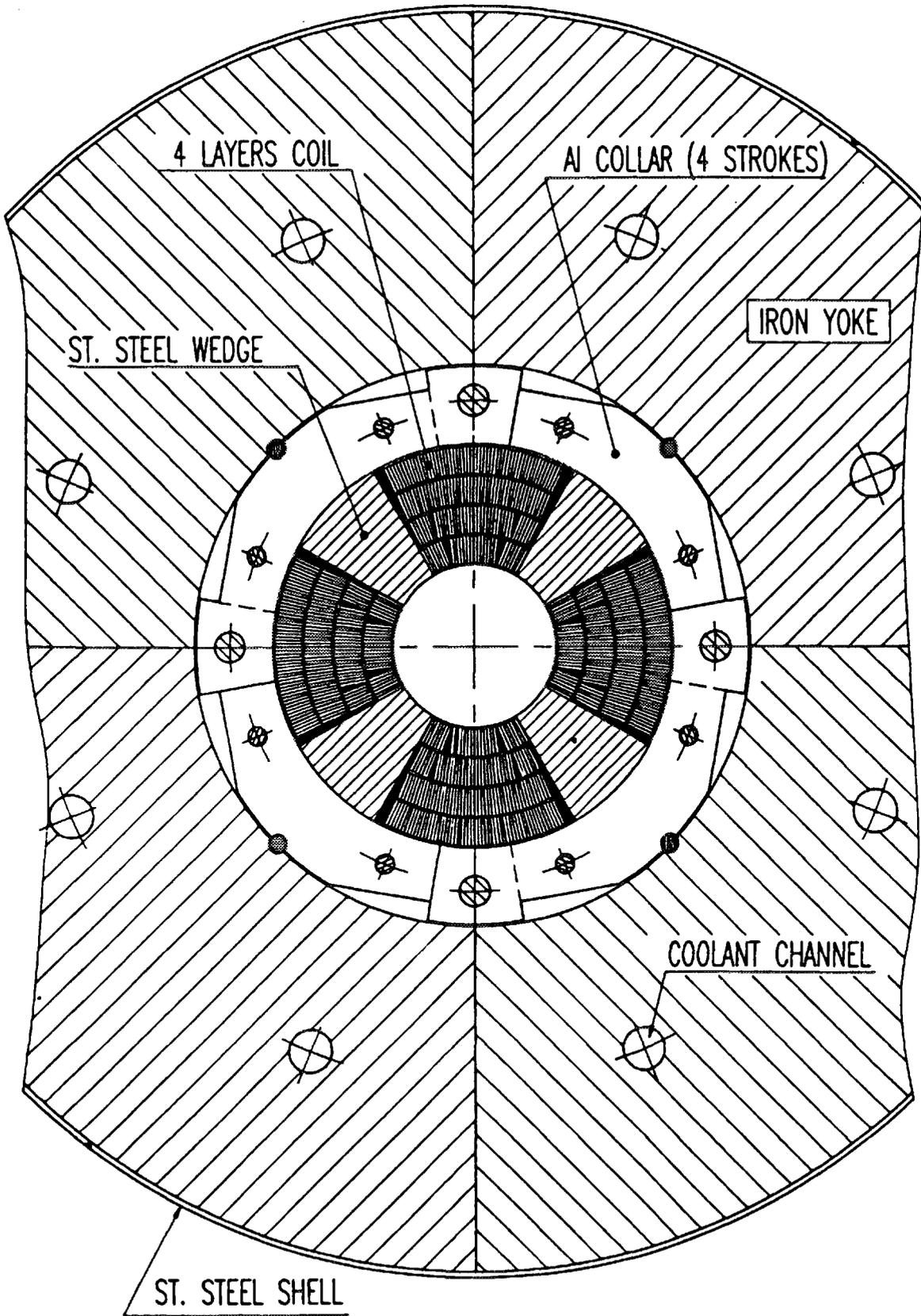
FIG. 11: cross section of the four shells magnet with the proposed ring-wedge collar system

designed press. In fig. 12 is reported an axonometric view of a home made press still in a preliminary design stage.
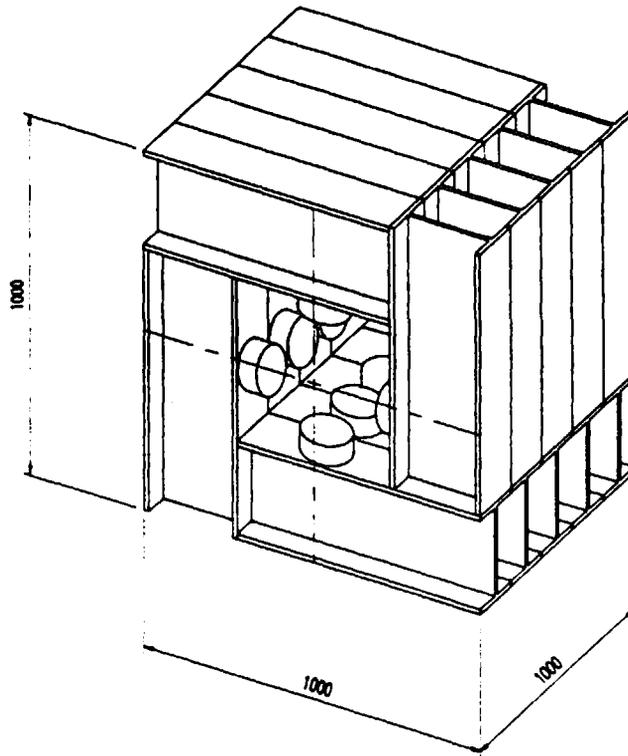
FIG. 12: axonometric view of the home made press to collar the magnet pushing along two perpendicular axes (dimensions in mm). Five hydraulic pistons can provide up to 150 ton, to a total of 750 ton/m in both directions.

In fig. 13 it is shown how the press acts on each collar quadrant: the force F_p applied by the press splits at a special angle of 55° thus providing the needed radial force and the wanted strain on the collar. Effectively the stretching of the collar is the most important feature of our collaring, thus helping to minimize the applied force with respect to the actual remaining stress in the coils as pointed out by M.Bona[16] .

The prestress due to collaring is very important because it must be high enough to avoid the detachment of coil upper edge from collar, but it must be not too high to avoid an excessive stress of the cables on midplane when the magnet is energized. In table 5 there are shown the minimum average prestress necessary to avoid coils detachment for some models, and also the resulting forces between coils and collar wedge after collaring.

On the design based on the 2S+2S coil layout it can be evaluated the benefit of the ring-wedge collar type: the needed prestress to be applied is decreased of 30% passing from the single collar made out of Aluminum alloy to the ring(Al-alloy)-wedge(Ti-alloy) design.

Looking at the 4 shell design, the one requiring the largest force acting on each coil, 3 MN/m, we worked out that for collaring by quadrant we need at least 4 MN/m with the best pushing angle of 55° . The proposed home made press, capable of a maximum 7.5 MN/m in both directions, seems adequate and able to take into account the friction effect (difficult to calculate and by experience evaluated about in 20-25% of the needed force, [16]) and uncertainty in the computation and material property.

If a dipole press is to be used, pressing in one direction, the 3 MN/m force on the each coil, request a pressing force of 6 MN/m. When friction is taken into account
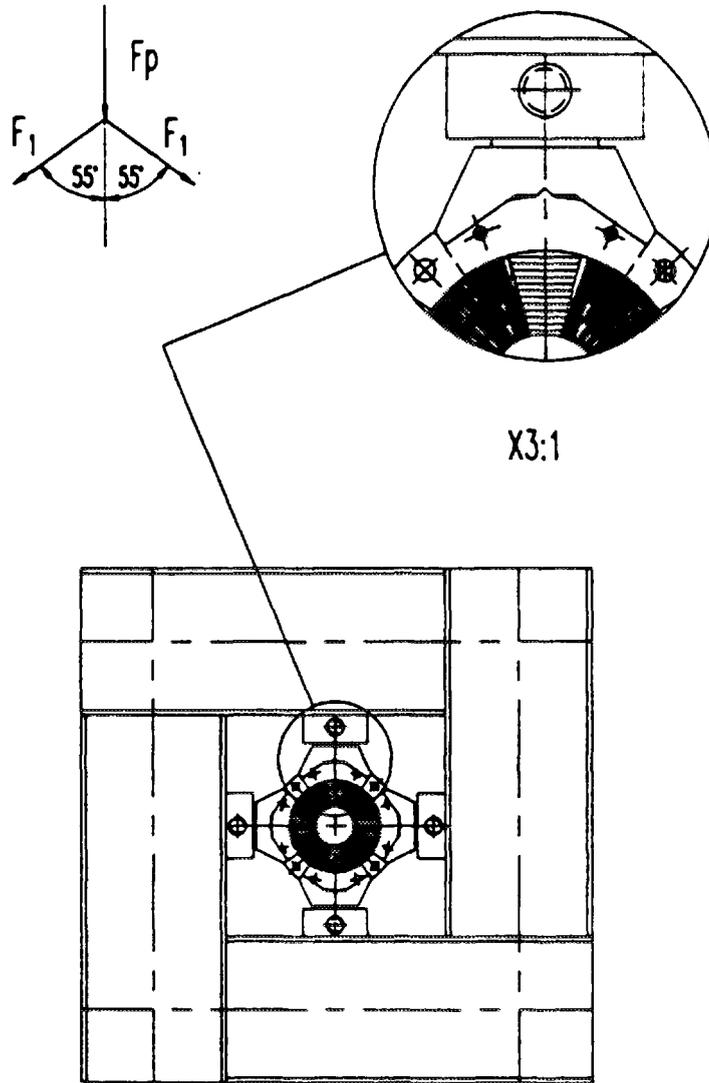
FIG. 13: collaring process by quadrant with the proposed press

together with an extra margin for contingency, we end up to about 7.5 MN/m as press capability.

The mechanical design has been carried out by means of ANSYS code and in figures 14,15 and 16 are reported the coil stresses after collaring, after cool down and at maximum current for the proposed 2S+2S design with ring-wedge collars. The maximum stress on the collar itself is acceptable, reaching the reasonable value of 350 MPa during collaring and 200 MPa in operation. This is again a benefit of splitting the collars.

It is worthwhile to remark that although the mechanical analysis is at a very preliminary step and need much detailed investigation, nevertheless any idea, concept and number have been checked with experienced magnet manufacturers[1].

[1] So far, coil stresses have been studied without any friction. Some simulations with infinite friction (i.e. no sliding) between coils and the wedge of the collar have shown an increase (10-15 %) of the maximum stress in coils with respect to the cases with no friction. This is due to a small elliptical coil deformation.

TABLE 5: coil prestress and pressing force on each coil

coil layout	collar type	ring radial size (mm)	wedge material	av. azimuthal prestress (MPa)	Force/coil (MN/m)
2 shells	single (Al)	20	=	54	1.6
2 shells	ring (Al)	20	Al	62	1.85
2 shells	ring (Al)	20	St. steel	53	1.6
2 shells	ring (Al)	20	Ti	53	1.6
2S + 2S	single (Al)	40	=	61	3.7
2S + 2S	ring (Al)	40	St. steel	48	2.9
2S + 2S	ring (Al)	40	Ti	44	2.65
4 shells	ring (Al)	40	Ti	50	3.0

As far as the coil end region, which has been voluntarily skipped, we think that the experience which has been gained with the dipole prototype and the information that CERN is getting by the investigation going on in its laboratory , will enable us to carried out a proper design. Collaboration with S. Caspi, LBL, and S. Russenschuck, CERN, allows to exploit the advantage of interconnection between magnetic design computer codes and computer controlled 5-axes machine that allow precise manufacture of the coil end spacers.

5.4 Stability and Protection

5.4.1 Operating Margin and Heat Deposition by Radiation

The margin against energy released by perturbation is given by operation at 93% of the maximum current, defined as the intersection of the magnet load line, B=B(I) and the critical current line, $I_c=I_c(B)$, as measured on cable short samples. When translated in term of temperature margin, i.e. the difference between the transition temperature and the operating temperature, we find $\Delta T = 3.3$ K for 4S, 2.1 K for the 2S+2S and 4.1 K for 2S coil layout. The calculated temperature margin is sufficient for magnet stability. Our temperature margin is greater than the one of the main LHC dipoles, 1.2 K [17] , however our coils are fully impregnated and need larger temperature margin than the wet coil (like dipoles). Actually also the dipoles have the coil ends fully impregnated, nevertheless they are able to pass the 93% of the maximum current, so we think that our aim is realistic. Since the coils are impregnated the effect due to heat deposition by secondary radiation has been evaluated. The given level of 2.7 mW/cm^3 of peak power dissipated into the coils [14] does not increase significantly the temperature if at least one surface of each layers is cooled by the liquid.

A detailed calculation and a map of heat deposition is being carried out with the Fluka code [18] integrated with a transport of lost particles through the beam pipe and magnetic elements. The results will be checked with the corresponding calculation by CERN.
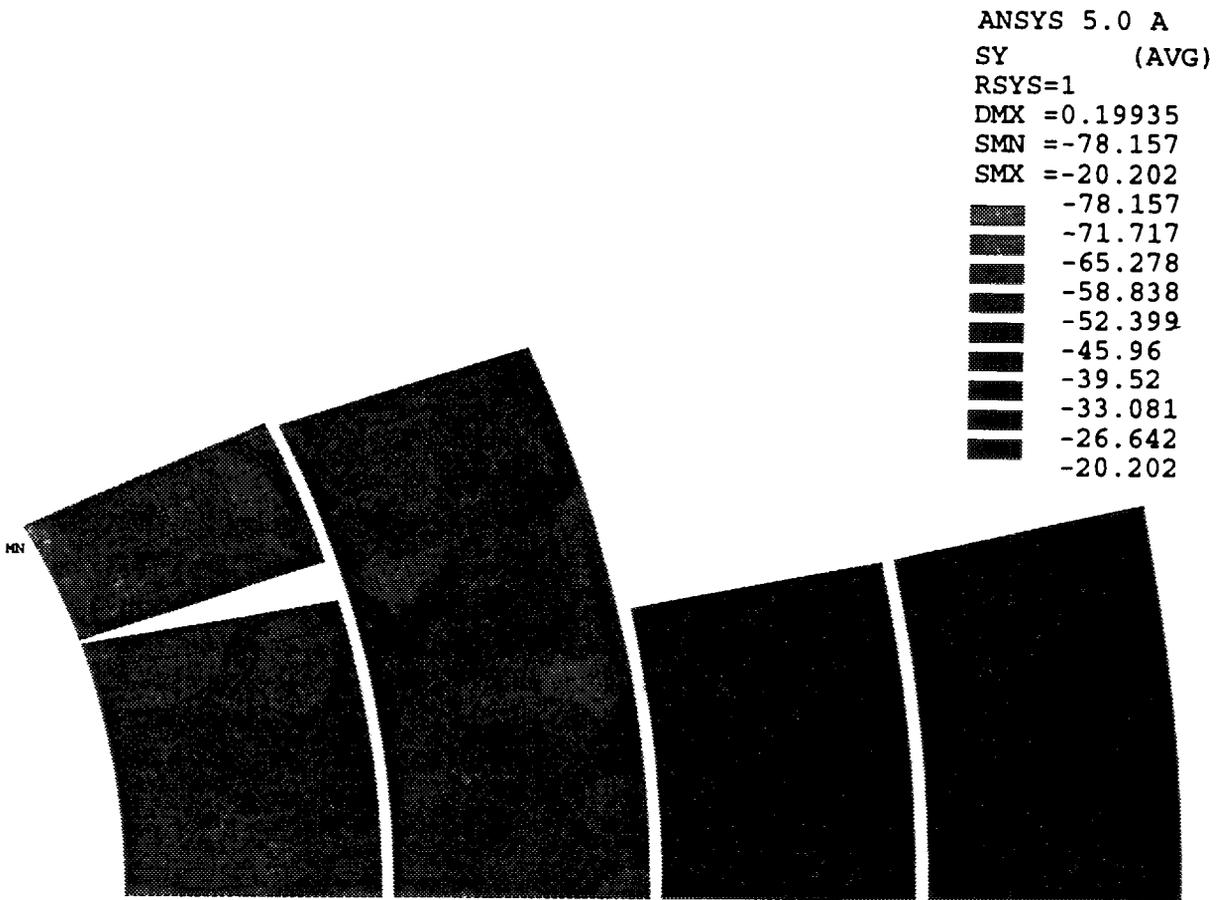
```
ANSYS 5.0 A
SY          (AVG)
RSYS=1
DMX =0.19935
SMN =-78.157
SMX =-20.202
        -78.157
        -71.717
        -65.278
        -58.838
        -52.399
        -45.96
        -39.52
        -33.081
        -26.642
        -20.202
```

FIG. 14: coil azimuthal prestress (MPa) after collaring.

5.4.2 Protection

The very high current density and the low copper fraction calls for an accurate quench analysis in order to work out the best protection system. At this stage we have modified a LASA code written for multicoil solenoids and we have used this for the preliminary investigation. The code deals with adiabatic magnet, fitting the case of this quadrupole that has full impregnated coils. Should the magnet be built, a detailed investigation will be carried in the frame of the CERN-INFN collaboration with a CERN code which is intended to deal specifically with accelerator magnets.

Since protection was envisaged to be an important issue for this magnet, a preliminary decision was to use a rather big cable for such a magnet, to avoid high inductance value. This allows to protect the 1 m long model with a single dumping resistor to be placed at the room temperature. At present we have investigated the scheme proposed in fig. 17.

For every layout the dumping resistor was fixed to a value giving 1.2 kV as a maximum voltage across the coil terminals. We judge this peak voltage still within the safety margin.

The behaviour of the maximum temperature (hot spot), of the magnet current, the voltage across the coil where the quench initiated and its resistance vs time are reported in figures 18 and 19 for all three layouts under considerations. The delay time
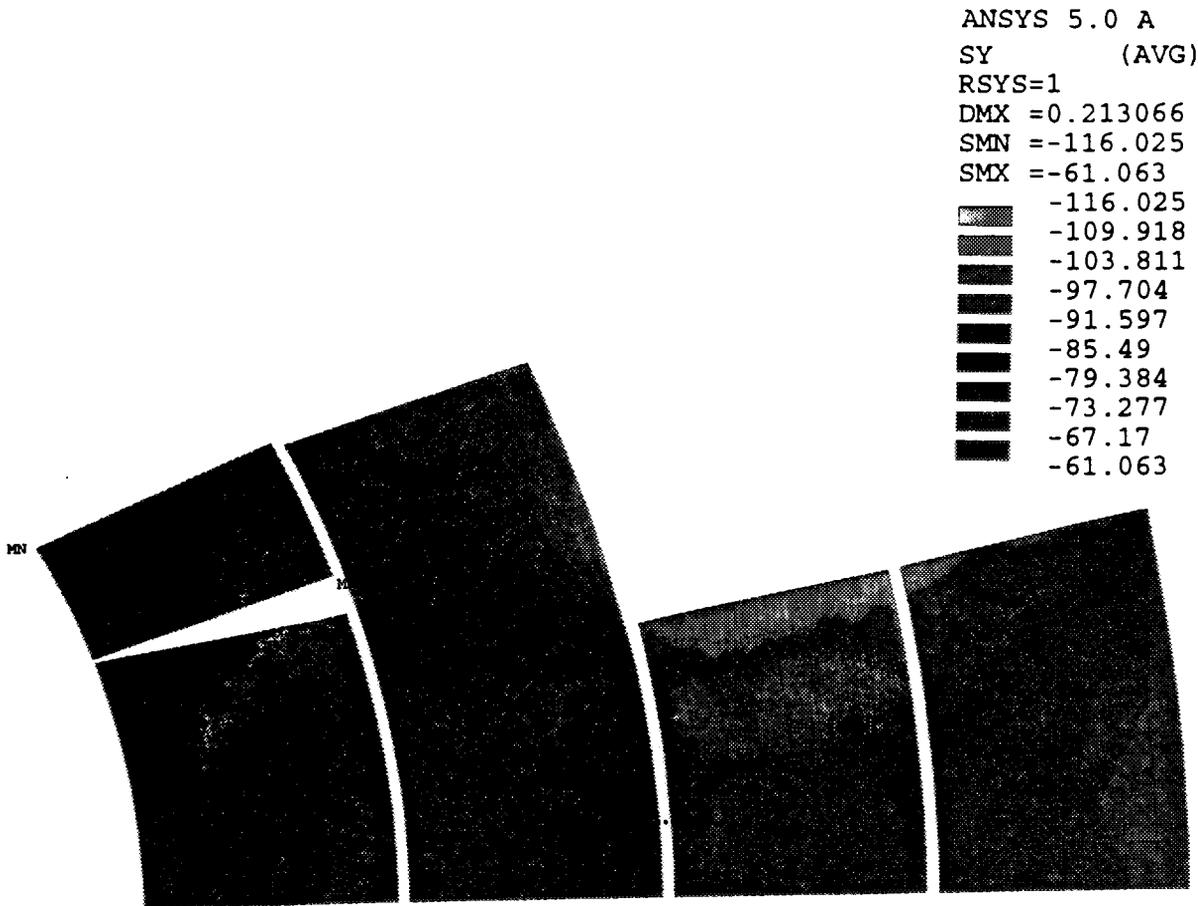
ANSYS 5.0 A
SY   (AVG)
RSYS=1
DMX =0.213066
SMN =-116.025
SMX =-61.063
          -116.025
          -109.918
          -103.811
          -97.704
          -91.597
          -85.49
          -79.384
          -73.277
          -67.17
          -61.063

FIG. 15: coil azimuthal stress (MPa) after cool down.

in quench detection has been fixed to 10 ms after a voltage threshold of 200 mV has been exceeded across one coil. An arc time (time actually needed to break the circuit) of 20 ms has been assumed.

Hot spot temperature is approximately 160 K for the 2S design and less than 190 K both for the 2+2 and the 4 shells coil layouts. Clearly the lower inductance of the 2 shells design allow to discharge the magnet quicker than in the case of the other designs but the higher current density will not tolerate any delay in discharging the magnet.

To check how critical is the delay time, we computed the maximum temperature vs the delay time in quench detection or the arc time of the switch. Results are reported in fig. 20 both for 4S and 2S. From this graph it is clear that while 2S has a lower hot spot temperature than the 4S with the standard detection and intervention time, 2S can get worse in case of longer delays, as pointed out when we commented the higher operating current of this coil layout.

We judge 200 K to be an acceptable temperature although at the limit of the system safety. We think it will be actually lower for the following reasons:

1. we have assumed a fairly large margin in the opening time of the mechanical switch, based on our previous experience with a 2500 A powering and protection system for a superconducting magnet. Actually the mechanical switch, even for 10-15 kA, can be faster. In the LHC dipole test station the mechanical

FIG. 16: coil azimuthal stress (MPa) at maximum current (G=257 T/m).
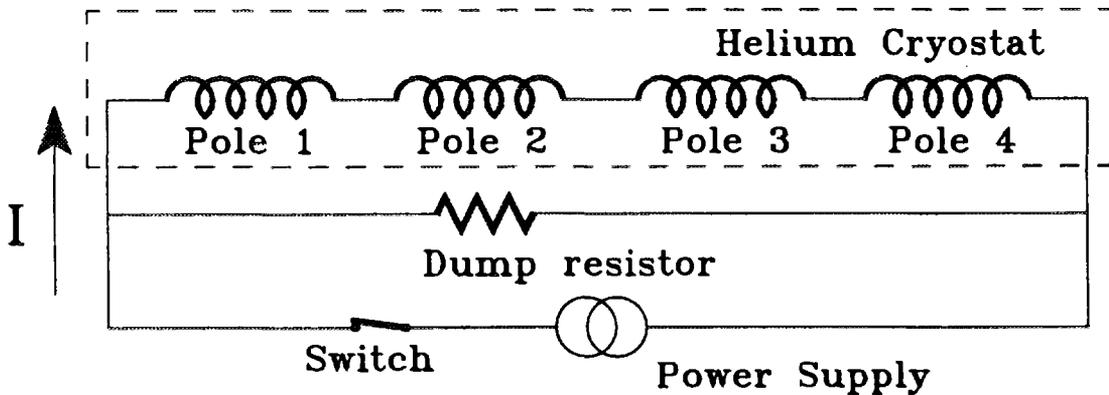

FIG. 17: electrical scheme of the magnet supply and protection system

switch opens in less than 10 ms and is considered the safety system since actually the circuit is broken by a solid state switch, a thyristor, which acts virtually instantaneously (less than 1 ms) and that, in hundred of tests, never failed [19];

2. no quench propagation enhancement due to fast field variation has been taken
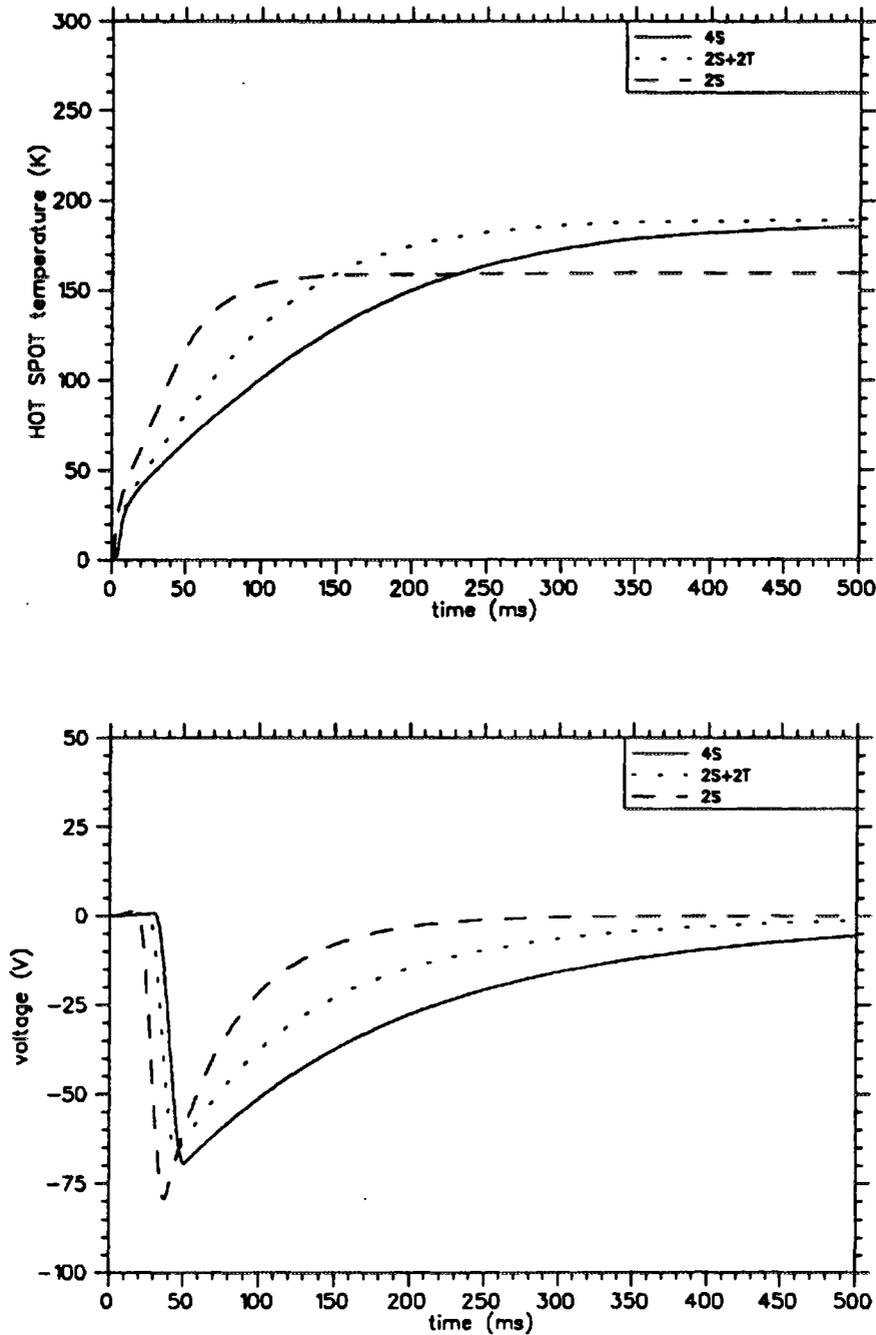
FIG. 18: hot spot temperature and voltage across the quenched coil vs time. Solid line: 4S, long dashes: 2S, short dashes: 2S+2T.

into account and no energy transfer to other metallic part. Especially the field variation effect, although difficult to evaluate precisely, should give a considerable help to the protection. We are not considering the use of active heaters because the time scale is very short, less than 300 ms, and makes externally activated quench heaters, less effective than they are in the dipole magnet;

3. possibility to shunt every coil with a resistor inside the cryostat. This solution, while very effective in lowering the hot spot temperature, looks complicated for a 1 m long model because requires space to allocate 15 kA diodes in series to the
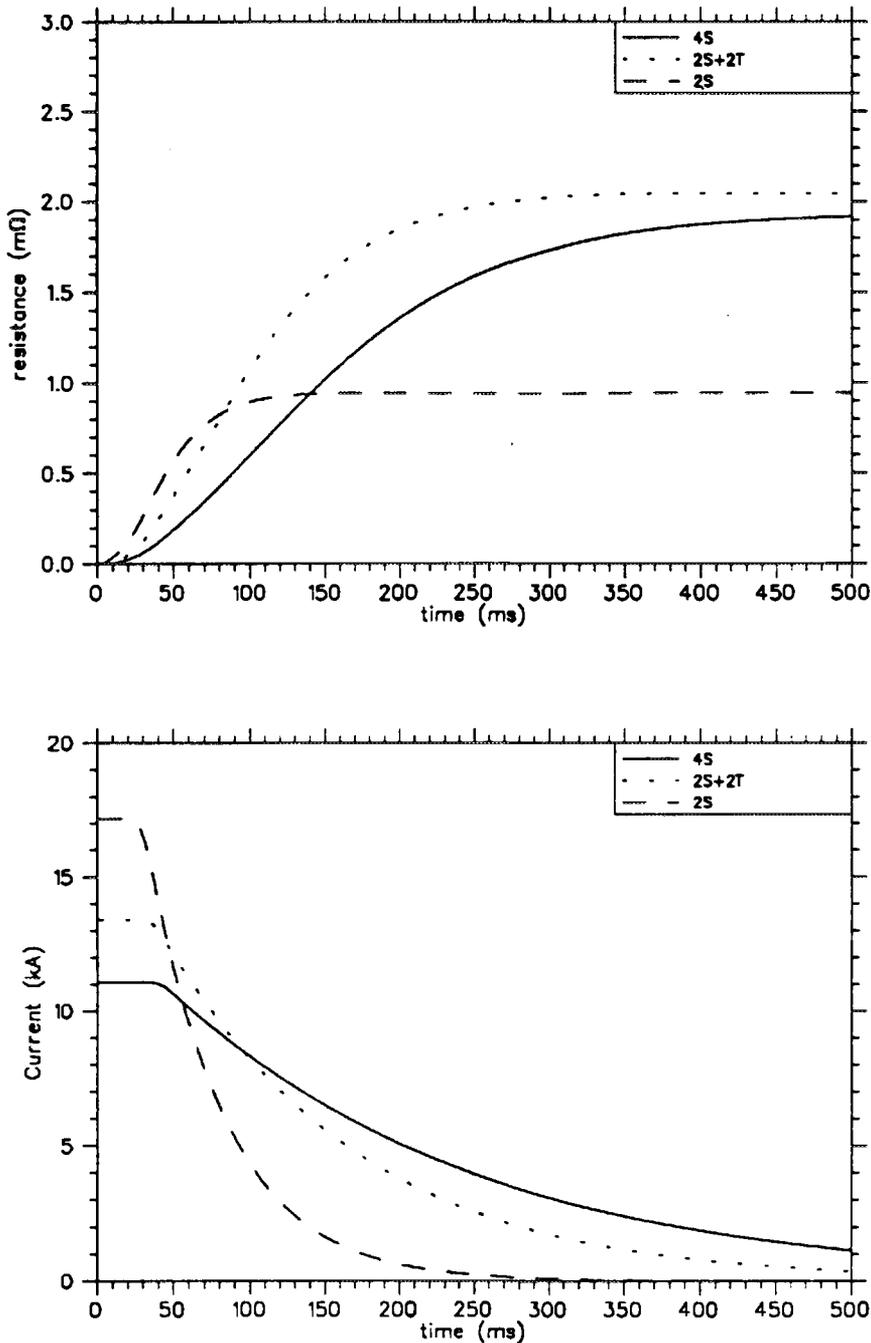
FIG. 19: resistance of the quenched coil and magnet current vs time. Solid line: 4S, long dashes: 2S, short dashes: 2S+2T.

shunt resistors.

The externally activated quench heaters and coil sectioning with shunt resistors will be probably necessary for the real 5 m long magnets.

To understand the effect of the most important quench parameters it's useful to evaluate the trade-off between maximum temperature (which requires high dumping resistance) and maximum acceptable voltage in the magnet (which requires low dumping resistance). Results are shown in fig. 21, showing that if 1.5 kV can be sustainable with safety, the temperature is well below the danger threshold.
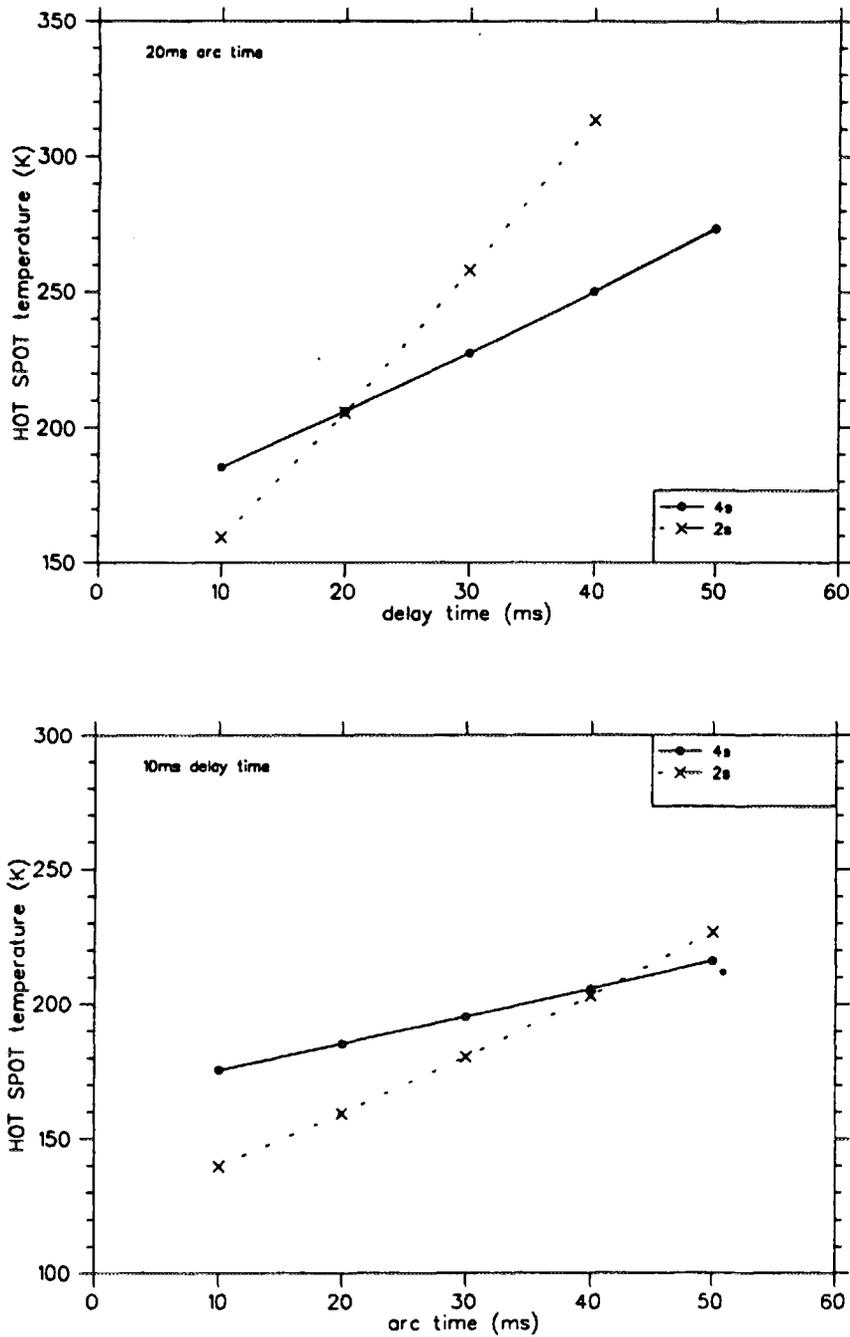
FIG. 20: hot spot temperature vs delay time (top) and vs arc time (bottom) for the 4S (dots) and 2S (crosses)

6 CONCLUSIONS

Most of the conclusions have been anticipated in the summary at the beginning of the proposal. List of parameters, cost and time schedule are reported in the summary.

Here it is worth to point out that the three designs have been analysed in terms of magnetic design, stress and protection and all three look feasible.

Focus has been on 2S design and on 4S one. Feasibility of the latter has been studied with more details from the mechanical point of view since it is more difficult. The 4S design is at present not yet optimized for the coil design.
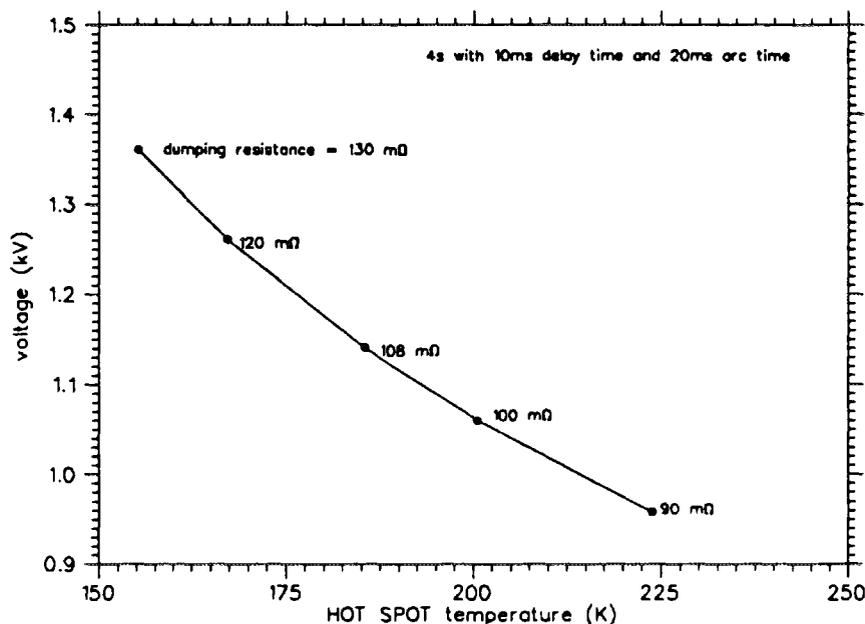
FIG. 21: Hot spot temperature vs maximum voltage across terminals for the 4 shells design

The four shells design is surely the most appetizing if final performance are the dominating goal. In our opinion there is room for better efficiency and for increasing of cable performance within one year: it is quite possible that actually *a 280 T/m gradient (still at 93% of the nominal maximum) in a 85 mm aperture* can be reached with this design after a detailed optimization.

The two shell design has lower gradient than the other two options, however it should be pointed out that to make this magnet all problems typical of Nb_3Sn and of this kind of high gradient large aperture quads are encountered. Because the development of Nb_3Sn technology is one of the main aims and since for long magnets two layer coils are more suitable for safety and cost consideration, *we prefer to start the project with the 2S, two shells coil design, aimed to 240 T/m in a 85 mm coil aperture.*

7 ACKNOWLEDGEMENTS

REFERENCES

(1) R. Perin, "Status of the LHC Magnet Development", MT-13 Conf., Victoria B.C., September 1993

(2) D.Dell'Orco et al., "A 50 mm Bore Superconducting Dipole with a Unique Iron Yoke Structure", Presented at ASC, Chicago August 1992

(3) R. Perin, "State of the Art in High Field Superconducting Magnet for Particle Accelerators", Proc. of XIV Int. Conf. on High Energy Accelerators, Tsukuba (J) 1989

(4) R.McClusky et al., "A Nb$_3$Sn High Field Dipole" IEEE Trans. on Mag. Vol.27, N.2, March 1991, p.1993

(5) A.Asner, R.Perin, S.Wenger, F.Zerobin, "First Nb$_3$Sn 1m Long Superconducting Dipole Model Magnet for the LHC Break the 10 Tesla Field Threshold, Proc. of MT-11 Conf. Tsukuba 1989, pag. 36

(6) D.Dell'Orco, R. Scanlan, and C.E.Taylor, "Design of the Nb$_3$Sn Dipole D20", Presented at ASC, Chicago, August 1992

(7) S. Caspi, "High Field Nb$_3$Sn Superconducting Dipole Magnets" SC-MAG-489, LBID-2079, January 1995.

(8) H.H.J. ten Kate et al. "Development of a 10 T Nb$_3$Sn Twin Aperture Model Dipole Magnet for the CERN LHC", Proc. of MT-11 Conference, Tsukuba 1989, pag. 66
A. den Ouden et al., " An Experimental 11.5 T Nb$_3$Sn LHC Type of Dipole Magnet", Proc. of MT-13 Conf., Victoria B.C., 1993, pag. 2320.

(9) T.M.Taylor, R.Ostojic, "Conceptual Design of a 70 mm Aperture Quadrupole for LHC Insertions", Proc. of ASC '92 and Internal Note CERN AT/92-24 (MA)

(10) R.Ostojic, T.M.Taylor, G.A.Kirby, "Design and Construction of a One-Metre Model of the 70 mm Aperture Quadrupole for the LHC Low-β Insertions", Proc. of MT-13, pag.1750

(11) N.Galante and T.Taylor, "Design Study of a Quadrupole Made with Rectangular Coil Blocks", draft of Internal Note CERN-AT/MA

(12) G. Ambrosio, G. Bellomo and L. Rossi, "Study of a High Gradient, Large Aperture, Nb$_3$Sn Quadrupole for the lowβ Insertions of the LHC", Proc. of EPAC 1994, London, pag.2268.

(13) G. Ambrosio, F. Ametrano, G. Bellomo and L. Rossi, "Computation of Magnetic Field, Multipole Expansion, Peak Field for Coil Dominated Accelerator Magnets by means of Complex Analysis", to be published as INFN report.

(14) T. Taylor, CERN-AT/MA, private communication, 1994.

(15) S.Russenschuck, "ROXIE, the Routine for Optimization of magnet X-section, Inverse problem solving and End region design", LHC note 238 1993, CERN-AT/MA
S. Russenschuck, "A Computer Program for the Design of Superconducting Accelerator Magnets", Invited paper at 11th Annual Review of Progress in Applied Computational Electromagnetics, March 20-24, Monterey (Ca), USA

(16) M. Bona, CERN-AT/MA, private communication, 1995

(17) The LHC Accelerator Project, CERN/AC/93-03(LHC), edited by Y.Baconnier, G. Brianti, Ph.Lebrun, A.Mathewson, R.Perin

(18) A. Fassò, A. Ferrari, J. Ranft and P. R. Sala, "FLUKA: present status and future developments", Proceedings of the IV International Conference on Calorimetry in High Energy Physics, La Biodola (Elba), September 19-25 1993, A. Menzione and A. Scribano eds., World Scientific, p. 493 (1994).

(19) D. Hagedorn, CERN-AT/MA, private communication, 1995